CR 137966

ADDITIONAL EXPERIMENTS WITH A FOUR-BLADED CYCLIC PITCH STIRRING MODEL ROTOR

Part II of Second Yearly Report under Contract NAS2-7613

Prepared for the Ames Directorate, USAAMRDL
at Ames Research Center, Moffett Field, California

by

K. H. Hohenemser

and

S. T. Crews

Department of Mechanical Engineering

Washington University
School of Engineering and Applied Science
St. Louis, Missouri 63130

(NASA-CR-137966) ADDITIONAL EXPERIMENTS WITH A FOUR-BLADED CYCLIC PITCH STIRRING MODEL ROTOR, PART 2 OF SECOND YEARLY REPORT (Washington Univ.) 70 p HC A04/MF A01 CSCL 01A

N77-10006

Unclas G3/02 08054

June 1975

CR/137966

ADDITIONAL EXPERIMENTS WITH A FOUR-BLADED CYCLIC PITCH STIRRING MODEL ROTOR

Part II of Second Yearly Report under Contract NAS2-7613

Prepared for the Ames Directorate, USAAMRDL
at Ames Research Center, Moffett Field, California

by

K. H. Hohenemser

and

S. T. Crews

Department of Mechanical Engineering

Washington University
School of Engineering and Applied Science
St. Louis, Missouri 63130

June 1975

Preface to Second Yearly Report under Contract NAS2-7613

Work under Contract NAS2-7613 started on July 1, 1973 as a continuation of research conducted under Contract NAS2-4151 since February 1, 1967. The research goals stated in Contract NAS2-7613 are

(a) Assess analytically the effects of fuselage motions on stability and random response. The problem is to develop an adequate but not overly complex flight dynamics analytical model and to study the effects of structural and electronic feedback, particularly for hingeless rotors.

(b) Study by computer and hardware experiments the feasibility of adequate perturbation models from non-linear trim conditions. The problem is to extract an adequate linear perturbation model for the purpose of stability and random motion studies. The extraction is to be performed on the basis of transient responses obtained either by computed time histories or by model tests.

(c) Extend the experimental methods to assess rotor wake-blade interactions by using a 4-bladed rotor model with the capability of progressing and regressing blade pitch excitation (cyclic pitch stirring), by using a 4-bladed rotor model with hub tilt stirring, and by testing rotor models in sinusoidal up or side flow.

Work on research goal (a) has been reported in Part I of the First Yearly Report under subject contract titled "Methods Studies Toward Simplified Rotor-Body Dynamics". The results were published in the paper: Hohenemser, K. H. and Yin, S. K., "On the Use of First Order Rotor Dynamics in Multiblade Coordinates" presented at the 30th Annual National Forum of the American Helicopter Society, May 1974, Preprint 831.

Initial work on research goal (b) has been reported in Part II of the First Yearly Report under subject contract titled "Computer Experiments in Preparation of System Identification from Transient Rotor Model Tests".

Initial work on research goal (c) has been reported in Part III of the First Yearly Report under subject contract titled "Experiments with a Four-Bladed Cyclic Pitch Stirring Model Rotor."

The second Yearly Report under Contract NAS2-7613 is subdivided into two parts, whereby Parts I and II are related to the research goals (b) and (c) respectively. The authors and titles of the two parts are:

Part I Hohenemser, K. H., Banerjee, D. and Yin, S. K., "Methods Studies on System Identification from Transient Rotor Tests."

Part II Hohenemser, K. H. and Crews, S. T., "Additional Experiments with a Four-Bladed Cyclic Pitch Stirring Model Rotor."

Part I begins with an introduction to aircraft/identification methods, it contains the results of computer experiments with several selected methods of system identification applied to lifting rotors, and contains the development of a new method for optimal data utilization.

Part II presents extended frequency response measurements with the four-bladed model rotor including dynamic wake measurements at zero advance ratio. It describes the modifications of the model and its instrumentation for transient pitch stirring tests, and it discusses the development of software for the data processing.

IV

ADDITIONAL EXPERIMENTS WITH A FOUR-BLADED CYCLIC PITCH STIRRING MODEL ROTOR

Part II of Second Yearly Report under Contract NAS2-7613

ABSTRACT

The frequency response tests with the 4-bladed pitch stirring rotor model, reported in Part III of the First Yearly Report under Contract NAS2-7613, have been extended to a rotor dynamic wake survey at zero advance ratio, covering 2°, 5° and 8° collective pitch settings. Dynamic wake data are taken in planes .12 and .20 radii below the rotor disk. These data are later to be compared with analytical wake data with parameters to be identified from pitch stirring transients. The model has been modified to perform such transients. The instrumentation developed for this purpose is described together with the method of data acquisition and with the test procedures. The hardware and software for several data handling systems is discussed. These systems have the purpose to extract from pitch stirring transients the parameters of analytical dynamic rotor wake models. The test data from pitch stirring transients at zero advance ratio have been acquired but not as yet processed.

TABLE OF CONTENTS

INTRODUCTION

The results of the frequency response tests with the 2 and 4 bladed pitch stirring rotor models presented in Part III of the First Yearly Report under Contract NAS2-7613 showed particularly at zero and low advance ratio large effects of the dynamic rotor wake on the blade flapping response. Only a few spotty dynamic wake measurements had been made at that time at zero advance ratio. It was found that when pitch stirring frequency and flapping natural frequency coincide, the dynamic wake amplitude .2 R below the rotor plane and .82 R from the rotor axis is almost zero. The ground plane is located 1.3 R below the rotor plane and should have little effect on this result. The dynamic wake amplitude was found to increase steeply when the blade natural flapping frequency was increased with respect to the pitch stirring frequency. To shed some more light on this interesting dynamic rotor wake behavior, it was decided to obtain at zero advance ratio a complete wake survey closely below the rotor plane extending over the entire radius and including 3 collective pitch settings of 2°, 5°, 8°. The first section of this report presents the results and a discussion of these results.

The goal of the dynamic rotor wake work is to find an analytical dynamic rotor wake description that is fitted by parameter identification from transients to best represent the wake effects on blade flapping responses. For this purpose the rotor model was modified to accept pitch stirring transients. The analytical wake description makes use of multiblade coordinates. Instrumentation and data acquisition had to be adapted to this requirement. Finally, the parameter identification algorithms which have been practiced and developed in computer simulations, require suitable data handling systems. Several possibilities of such systems are open. The associated software had to be developed. The last section of this report discusses this problem.

DYNAMIC ROTOR WAKE SURVEY FROM FREQUENCY RESPONSE TESTS AT ZERO ADVANCE RATIO

The frequency response tests presented previously were performed either with the 2-bladed rotor model of 16 inch diameter, or with the 4-bladed rotor model of 16.5 inch diameter. The tests covered advance ratios from 0 to .74 and collective pitch angles of 2° and 5°. For most of the tests only flapping responses were measured. For zero advance ratio also the time variable downwash at one point under the rotor plane was recorded with a hot wire anemometer. The extended work reported in the following provides dynamic rotor downwash measurements at zero advance ratio over the entire rotor radius in 2 planes below the rotor disk.

1. Test Conditions

Two test series were conducted. In the first series the rotor speed was 120 ft/sec or 27.5 cps resulting in a non-dimensional blade natural frequency in the rotating system of P = 1.17. This test series was conducted only with 4 blades set at collective pitch angles of θ_o = 2°, 5°, 8°. The second test series was conducted both with 2 and 4 blades set at 2° collective pitch angle. Two rotor speeds were used corresponding to P = 1.25 and 1.175. The 2-bladed rotor model was obtained by removing 2 blades from the 4-bladed rotor model. The ground plane was in all tests 1.3 R below the rotor center.

The rotor characteristics are the same as in the earlier tests, except that now the 2-bladed rotor has half the blade solidity ratio of the 4-bladed rotor. Diameter D, blade solidity ratio σ, first and second natural blade flapping frequency, non-rotating ω_{β_1}, ω_{β_2}, first blade torsional frequency ω_{θ_1}, first blade chordwise frequency ω_{ζ_1}, Lock number γ, and pitch stirring amplitude θ_c are

D inches	σ	ω_{β_1} cps	ω_{β_2} cps	ω_{θ_1} cps	ω_{ζ_1} cps	γ	θ_c°
16.5	.154(.077)	14.0	166	180	114	4.2	1.50

The cyclic pitch stirring frequencies, as determined by the available gear ratios, are in rotating coordinates

.20 .40 .60 .80 .90 .933 1.067 1.10 1.20 1.60 1.80

For the first test series with 4 blades, θ_o = 2°, 5°, 8°, P = 1.17, two single channel linearized hot wire anemometers were used for the velocity measurements, located .20 R and .12 R below the rotor plane. For the second test series with 2 and 4 blades, $\theta_o = 2°$, P = 1.25 and 1.175 only one hot wire anemometer .20 R below the rotor plane was installed. Figure 1 shows the 7 probe locations along the radius.

2. Test Results

For the first test series with the 4-bladed rotor at P = 1.17 and $\theta_o = 2°, 5°, 8°$ three characteristics are presented. The time average of the rotor downwash velocity $\overline{w}$, the time mean square of this velocity $(\overline{w^2})^{1/2}$, and the absolute value of the first Fourier coefficient with respect to the pitch stirring frequency $|F_{1\omega}|_w$. Each characteristic is plotted in two ways. Figures 2a to 10a show the 3 quantities plotted versus excitation frequency in the rotating system ω with the radial station r/R as parameter. Figures 2b to 10b show the 3 quantities plotted versus radial position r/R with the excitation frequency ω as parameter. Some of the plots give the data for the probe location .20 R below the rotor center, some for .12 R probe location and some for both locations. In most cases the differences in the characteristics between these 2 probe locations are small.

The time averages shown in figures 2 to 4 for .20 R probe locations were obtained by manually recording the readings of a time averaging DC voltmeter as the tests were in progress. The time root mean square values in figures 5 to 7 for both .12 R and .20 R probe locations were obtained by playing back the tape recorded measurements through a RMS meter using one second as the integration interval.

Figures 8 to 10 show the mean and standard deviations of the absolute values of the first Fourier coefficients of the frequency response of the wake measurements taken at .12 R below the rotor plane. These values were obtained by playing back the tape recorded wake measurements through a PDP-12 computer which digitizes the measurements and Fourier analyses them 7 times with the frequency of excitation over 7 consecutive periods of excitation and then takes the mean and standard deviation of those 7 Fourier coefficients. These 3 curves represent approximately 25 hours of PDP-12 computer time. All three sets of data were put on punch cards and plotted with a Calcomp plotter.

The second set of tests with $\theta_0 = 2°$, 4 and 2 blades, P = 1.25 and 1.175 and probe locations .12 R below the rotor center was evaluated in a different manner by computing spanwise weighted averages of the 3 characteristics $\bar{w}$, $(\overline{w^2})^{1/2}$, $|F_{1\omega}|_w$. The first weighted average

$$(1/R^3) \int_0^R \ldots r^2 dr$$

is proportional to the hub moment from the downwash. The second weighted average

$$(1/R^2) \int_0^R \ldots r dr$$

is proportional to the rotor lift deficiency from the downwash.

Figures 11 and 12 show the weighted average

$$(1/R^3) \int_0^R \bar{w}\, r^2 dr$$

which is labeled "Hub moment from $\bar{w}$" though it is different from the actual hub moment by a constant factor. Figures 13 and 14 show the weighted average

$$(1/R^3) \int_0^R |F_{1\omega}|_w \; r^2 dr$$

which is labeled "Hub moment from $|F_{1\omega}|_w$" though it need be multiplied by a constant factor to obtain the actual hub moment.

Figures 15 and 16 show the weighted average

$$(1/R^2) \int_0^R \bar{w}\, r dr$$

which is labeled "Thrust Deficiency from $\bar{w}$," it again needs multiplication by a constant factor. Finally figures 17 and 18 show the weighted average

$$(1/R^3) \int_0^R (\overline{w^2})^{1/2} r^2 dr$$

which is labeled "Hub moment from $(\overline{w^2})^{1/2}$" whereby the constant factor is omitted. Each set of 2 figures gives the spanwise weighted averages for 2 and 4 blades and for blade natural frequencies of P = 1.25 and 1.175. In all figures 2 to 18 the ordinates have the dimension ft/sec and are plotted versus the pitch stirring frequency in rotating coordinates ω.

Figures 19 to 22 show the absolute value of the first Fourier coefficient of blade flapping $|F_{1\omega}|_\beta$ and the phase angle between excitation and response ϕ_{c1}. Figures 23 and 24 show the difference in flapping amplitude between the analytical (no wake) and measured flapping response. This difference is compared to the downwash hub moment amplitude. The scales are arbitrary.

3. Discussion

Figures 2 to 7 show that as the collective pitch increases both $\bar{w}$ and $(\overline{w^2})^{1/2}$ become less dependent on the pitch stirring frequency. This would be expected because of the larger values of thrust produced downwash as compared to the pitch stirring produced downwash. The first Fourier component $|F_{1\omega}|_w$ remains strongly frequency dependent for all collective pitch settings, see figures 8 to 10. This Fourier coefficient has always a minimum close to $\omega = 1.2$ where the pitch stirring excitation frequency in the regressing mode approximately coincides with the blade natural flapping frequency. The radial distribution of all 3 quantities $\bar{w}$, $(\overline{w^2})^{1/2}$ and $|F_{1\omega}|_w$ has always a maximum in the vicinity of r/R = .8. For the higher collective pitch settings the maximum tends to shift inboard, particularly for the wake amplitude $|F_{1\omega}|_w$.

From figures 11 and 12 it is seen that the spanwise average of the time mean $\bar{w}$ is frequency dependent both for the 2 and 4-bladed rotor. The reason is the non-linearity in the superposition of steady and unsteady downwash. The steady downwash originates in 2° collective pitch angle, while the unsteady wake has its source in 1.5° cyclic pitch stirring.

The mean wake for 4 blades is less than twice that for 2 blades, see figures 11 and 12. The hub moments of the dynamic wake amplitudes for 2 and 4-bladed rotors are relatively close to each other, see figures 13 and 14. This is also reflected in the flapping responses, figures 19 to 22 which show no substantial differences between 2 and 4-bladed rotors. The differences in peak values in figure 19 may have been caused by insufficient number of test points along the ω-axis in this frequency range and consequently a crude interpolation from computer graphics.

Figs. 23 and 24 show that the deviations between the analytical flapping response computed without unsteady wake effect and the actual response agree reasonably well with the measured unsteady hub moment, though the shift of the wake amplitude peak to higher frequencies seems to have no obvious explanation. It should be noted again that the graphs in figures 23 and 24 have arbitrary scales so that only their shapes, not their magnitudes should be compared. Also, because of insufficient number of test points, computer graphics distorted the curves in the vicinity of steep ascents or steep descents. By and large the similarity between the measured dynamic downwash hub moment amplitudes and the difference between analytical and measured hub moment response is evident and makes it plausible that this difference is caused by the neglect of the dynamic downwash in the analysis.

TRANSIENT PITCH STIRRING TESTS

Zero advance ratio transient pitch stirring tests using various stirring accelerations have been conducted with collective pitch angles of 2°, 5°, 8°. The test data have no' as yet been processed and are, therefore, not presented herein. Forward flight transient pitch stirring tests are being prepared. The test set-up and the test procedures are described in this section.

1 Generation of Transients

The following transients are generated with the 4-bladed pitch stirring model rotor:

(a)

$$\theta_I = 1.5 \sin (\omega_f t + \phi)$$

$$\theta_{II} = 1.5 \cos (\omega_f t + \phi)$$

Where the pitch stirring angular speed in fixed coordinates, ω_f, is a time function given by

$$\omega_f = 0 \quad , t \geqslant t_o$$

$$\omega_f = C(t - t_o)/\pi \quad , t > t_o$$

C can be varied between -.15 (progressing excitation) and +.15 (regressing excitation).

(b) $P = \infty$ to $P \geq 1.15$

$$\text{since} \quad P = \sqrt{1 + \frac{e}{R} + \left(\frac{\omega_{\beta_{\Omega=0}}}{\Omega}\right)^2}$$

and Ω goes from 0 to a constant speed in rotor start up. (e is the equivalent hinge off-set, $\omega_{\beta_{\Omega=0}}$ is the first flapping natural frequency, nonrotating).

(c) $\mu = 0$ to μ_{max} in wind tunnel start up.

Transient (a) is used for rotor parameter identification. Transients (b) and (c) are measured during testing but will not be currently used for the parameter identification.

Transient (a) is generated in the following way. There are motors which drive both the rotor shaft - which controls rotor azimuth angle, and the pitch shaft - which controls pitch azimuth angle. These motors are 1/2 horse 2 element variable speed motors. The primary element is a constant speed induction motor; henceforth referred to as the motor (rotor motor, pitch motor). The secondary element is a magnetic clutch, henceforth referred to as the clutch (rotor clutch, pitch clutch), that engages the variable speed drive shaft. By varying the current to the clutch (with the motor on), the drive shaft speed can be varied. Pitch transients are achieved by switching on the pitch clutch to a predetermined current level, with the motor running, and letting the shaft accelerate toward steady-state. Before steady-state is reached the pitch clutch is usually shut off and the shaft then decelerates.

Progressing and regressing pitch stirring tests using five different pitch acceleration values were conducted for collective pitch settings of 2°, 5° and 8°. The acceleration range brackets the acceleration value used in the identification similation tests.

2 Instrumentation and Calibration

Each blade flexure is instrumented with 4 strain gages, figure 25. For the zero advance ratio pitch stirring tests, the gages from opposing blades were wired into 2 Wheatstone bridge circuits so that $\beta_1 - \beta_3$ and $\beta_2 - \beta_4$ could be measured. Excitations to the 2 bridges and output signals from the 2 bridges were conducted through the 12 ring slip ring assembly. Calibration of the circuitry was accomplished by loading each blade with a known moment and reading the voltage level output. It was found that the voltage level outputs of opposing blades to the same moment matched to within less than 1.5 percent.

In forward flight pitch stirring tests the 4 strain gages on each blade will be wired into a Wheatstone bridge circuit that cancels torsion and edgewise moment contributions to the bridge imbalance. The flapping moment of each blade will be measured independently. An attempt was made to use the current 12 ring assembly with existing amplifier circuitry by supplying power to all bridges from one amplifier and by amplifying each bridge output separately. However, it was impossible to eliminate all of the cross-channel feedbacks. Consequently, at least a 16 slip-ring assembly is required. A 20 slip-ring assembly has been purchased and is being installed.

Resolvers are used to measure rotor and pitch stirring azimuth angle. The resolvers are mounted on independent shafts and are driven by a 2 to 1 timing belt and sprocket arrangement, so that the resolvers complete two cycles during one shaft revolution. The resolvers used are A.E.I. Model #II IR11N16138's. These resolvers were designed to be driven by a carrier frequency of 400 cps. At that carrier frequency, the resolvers indicate angular position by a sine function to within 1%. A much higher carrier frequency is used in the current test set up so that the low pass filter which filters out the rectified carrier will not significantly phase shift frequencies under 60 cps. When these resolvers are used in this manner, the accuracy of the sine function slips to lower than 20%. The angular position is no longer represented by a sine function, but by a smooth function that differs in a regular way from a sine function. This discrepancy is compensated for by programming.

For the zero advance ratio tests the rotor downwash was measured with 2 channel hot-wire anemometry at two points 90° apart. The probes were located at the 7 radial position shown in figure 1 .20 R and .12 R below the rotor at azimuth angles of $\psi = 0°$ and $\psi = 270°$. The probes were selected to be suitable for the wake frequency response measurements.

3 Data Acquisition

Real time data acquisition is performed on an Ampex 6 channel F.M. tape recorder. In the zero advance ratio tests the data recorded were rotor and pitch azimuth angle, $\beta_1 - \beta_3$, $\beta_2 - \beta_4$, and the two downwash measurements. In forward flight, the resolver information will be recorded as well as β_1, β_2, β_3, and β_4 (Table 1).

4 Testing Procedure

Table 1 shows a summary of the test procedures used for the zero advance ratio pitch stirring transients. They are discussed in more detail in the following.

Test Initialization

In previous reports it has been shown that the β calibration is independent of rotor velocity. The rotor blades are easily removed from the rotor root flexures. The unloaded flexure bridge output gives the true voltage level at $\beta = 0$; call this $\beta_{unloaded}$. Fixing the blades to the root flexure and taking a new measurement yields β_{loaded}. Thus $\beta_{adjust} = \beta_{unloaded} - \beta_{loaded}$ is the constant quantity that must be added to the measured β_{loaded} value, that is recorded before each test, to determine the real voltage level at $\beta = 0$. β_{adjust} need only be determined once for each blade.

$\theta_o = 0$ is determined by individually adjusting each blade pitch angle until $\beta_{unloaded\ \Omega = 0} = \beta_{loaded\ \Omega = \text{running speed}}$. This is possible because the β calibration is independent of rotor velocity.

Individual Test Calibration

Samples 1 through 3 are taken for test calibration purposes.

Test initialization procedures are shown in Table 1 under A. The rotor and pitch shaft are linked

Table 1

Test Procedure

Data Use:		calibration table & constants			raw data for processing	
tape channel #		Sample 1	Sample 2	Sample 3	Sample 4	Sample 5
Ch.1	Rotor resolver	1023 pts appr. 120 pts./rev.			Rotor Clutch start up triggers sampling. Collects 1024 pts. per channel.	Pitch Clutch starts up and triggers sampling. Collects 1024 pts. per channel.
Ch.2	Pitch resolver					
Ch.3	β_1 or $\beta_1-\beta_3$	1024 pts of 1.4 Volts	1024 pts of .4 Volts	1024 pts of loaded		
Ch.4	β_2 or $\beta_2-\beta_4$					
Ch.5	β_3 or $\psi=0°$					
Ch.6	β_4 or $\psi=270°$					

Tape Operations

6 ft (on – off) | on – off | on – 6 ft | 10 ft | 6 ft

A
1. link Shafts
2. Pitch clutch switch 1--on
3. Pitch clutch switch 2--on
4. Test voltage switch--1.4 V.
5. Rotor Motor switch--on
6. Rotor clutch switch--on

B
1. Rotor clutch switch--off
2. unlink shafts
3. Pitch clutch switch 1--off
4. Test voltage switch--.4 V.

C
1. Test voltage switch--off
2. Pitch motor switch--on

D
1. Rotor clutch switch--on

E
1. Pitch clutch switch 2--on

F
1. Pitch clutch switch 1--off
2. Rotor motor switch--off

tape speed -- 3 1/2 ips

together so that they run in tandem. A precise D.C. test signal of approximately 1.4 volts is fed to the tape channels that ultimately will record blade flapping. The switches on the pitch shaft motor clutch must be set as specified under A for the pitch resolver voltage to be fed into the tape Ch. 2. To rotate the rotor, the rotor motor and rotor motor clutch are engaged. After the rotor has reached the steady rotational speed required for the test, the tape recorder is turned on and information is recorded on 6 ft. of tape. The function of the sampling program which reads this section of tape is described in Table 1. The data collected on the resolvers is used to construct mappings from the azimuth angle-real waveform relation to an azimuth angle-sine wave relation for both resolvers. These two mappings are applied to all subsequent resolver data before parameter identification.

At B, the rotor is stopped, the pitch resolver disconnected, and a new precise D.C. test signal of approximately .3 volts is applied across the blade flapping channels. This information is recorded on 6 ft. of tape before rotor start up is initiated. The information obtained from sampling these channels is used to determine the true β_o.

Test Run

At D rotor start-up is initiated by engaging the rotor motor clutch. Since the rotor motor is already on, the rotor rapidly accelerates to the test speed. The rotor resolver channel is wired so that it records a 2 Volt signal until the rotor clutch is engaged, then the rotor resolver signal is engaged which varies between .2 and 1.8 volts. There is a voltage drop from 2 volts to the resolver signal level. This voltage drop is used by the sampling program to initiate data storage by the storage device. Thus one is sure of obtaining data from the very beginning of the transient. When the storage devices memory is full, sampling is stopped and data is normalized before the next sampling run. Sample 4 obtains data on transient P conditions. P goes rapidly from ∞ to its steady state conditions. At present there are no anlaytical programs available for using this data. This data is collected once for each Θ_0 condition. In wind tunnel testing a similar procedure will be used to collect transient advance ratio data.

At E pitch clutch switch 1 is engaged. This initiates the transient and initiates pitch resolver recording data collection which proceeds in the same manner as aforementioned. At F pitch clutch switch 2 is engaged. This terminates the transient acceleration, after which deceleration occurs, but does not terminate pitch resolver recording. Approximately 16 rotor revolutions at 60 pts/rev of data are collected per sample. If one finds that an important part of the transient occurs after 16 revolutions, one can delay data storage until the appropriate time by using the pitch resolver channel voltage drop as a clearly defined time point. After the transient has died away shutdown is initiated and the next test prepared.

Running 5 progressing and 5 regressing transients each at three collective pitch settings of 2°, 5°, 8° at zero advance ratio takes approximately 1 hour. This is only a small fraction of the effort required for frequency response tests.

DATA HANDLING SYSTEMS

After the desired transient pitch stirring tests have been conducted and the raw data have been recorded on the tape, three or four major data handling tasks must be accomplished. These tasks can be performed in a number of different ways depending upon the computer hardware and software available. The tests have been set up in such a way that they properly interface with the data handling tasks.

The first task to be accomplished is the conversion of the proper parts of the analog signals to digital form. The only part of the analog tape of interest is that very short section that contains the transient excitation and response. Collecting this section of data is initiated by triggering sampled data storage with a change in the pitching channel voltage level (Table 1). This task is accomplished on a PDP-12 computer at Washington University. The PDP-12 belongs to the family of minicomputers and has proven to be an effective laboratory computer. The PDP-12 on which this is done has:

1. 8,192 - 12 bit word core memory
2. 64,00 - 12 bit word DF32 random access disk storage space
3. 500,000 - 12 bit work RF08 fast random access disk storage space
4. 8 external analog-digital conversion channels

Assembly language programs have been written for obtaining the digitilized raw data. This data is temporatily stored on the DF32 d' ·k where it is sequentially addressed by data reduction programs.

A second possibility exists for achieving the data sampling task. A number of PDP-11 computers which have direct access to the University's IBM 360 computer have been installed around the campus. The PDP-11 is one of the new family of microcomputers. The basic processing cycle is about a third as fast as the PDP-12 processing cycle but is significantly cheaper and is tied to the main IBM computer. We have obtained access to two of these machines. The one with the best configuration has:

1. 28,000 - 16 bit word core memory
2. Virtually unlimited indirect disk storage (accessed through the IBM 360)
3. Interactive graphics display with hard copy capability

There is a good possibility that analog-digital conversion hardware will be added to one of these machines. Assembly language sampling software would have to be written to interface with the hardware as the available Fortran sampling subroutines are too slow. However, these programs are fairly straightforward to write.

Data Reduction is the second major task that must be accomplished. The digitilized data must be normalized with the proper normalization tables and constants which are constructed from calibration runs. Software for table construction and data normalization has been written and tested for both the PDP-11 and the PDP-12. These are Fortran II on the PDP-12 and Fortran IV (on the PDP-11) programs that read the data off the appropriate disk space (the DF 32 for the PDP-11), normalize the data, and rewrite the normalized data onto the appropriate storage device.

The last step in the data handling system is the identification analysis. Currently, the analysis can be done only on the IBM 360; consequently, one must either introduce normalized data transfer routines to get the data into the 360, or one must rewrite the identification analysis to fit the PDP-12 system. The only currently available method of transferring normalized data from the PDP-12 to the IBM-360 is by printing out the data and then key punching the data onto cards. This is a relatively laborious process and requires about one hour of key punching per transient. In the near future, an IBM compatible tape drive will be wired to the PDP-12 yielding yet another option to data transfer and handling.

Since the hardware for sampling data via the PDP-11 and/or writing data from the PDP-12 onto IBM compatible tape is not yet available, work is being directed at writing the identification analysis in PDP-12 compatible form. This task is complicated because of the small core memory available to the PDP-12 which makes it necessary to swap program segments into and out of core. A larger core memory would facilitate this task. The print-out and key punching routines can always be used as an alternate method if the identification analysis proves to be too big for the PDP-12 and none of the other options become available.

The ideal data handling system for sampling, data reduction and identification analysis would be the presently available PDP-12 system with an additional 24,000 words of core memory. This would enable one to do all necessary processing on the same machine, from start to finish. It would also allow for quick operator interaction with the processing routines. As has been stated, this flexibility can be achieved with the presently available system, however programming is more complicated than it would be for the extended memory system described above. Table 2 shows the present state of availability of the hardware and software for the various alternatives.

Table 2

Task	Machine	Presently Availible: Hardware	Presently Availible: Software
Data Sampling	PDP-12	yes	yes
	PDP-11		yes
Data Reduction	PDP-12	yes	yes
	PDP-11	yes	yes
Reduced Data Transfer into main computer	PDP-12 via magtape		
	PDP-12 via keypunch	yes	yes
	PDP-11	yes	yes
Identification Analysis	IBM 3[illegible]0	yes	yes
	PDP-12	yes ?	

CONCLUSIONS

In a survey of the dynamic rotor wake from steady 1.50° pitch stirring at zero advance ratio in planes .12 R and .20 R below the rotor center, using 2°, 5°, 8° collective pitch and blade natural flapping frequency when rotating of P = 1.17 the following characteristics were found:

1. The spanwise distributions of the time average $\bar{w}$, of the time root mean square average $(\overline{w^2})^{1/2}$ and of the absolute value of the first Fourier coefficient with respect to the stirring frequency $|F_{1\omega}|_w$ have a maximum at about .8 R. For the higher collective pitch angles this maximum has the tendency to shift inboard, particularly for the wake amplitude $|F_{1\omega}|_w$.
2. The time average $\bar{w}$ and the time root mean square average $|\overline{w^2}|^{1/2}$ becomes less variable with pitch stirring frequency, as the collective pitch increases.
3. The wake amplitude $|F_{1\omega}|_w$ is strongly dependent on the pitch stirring frequency. It is almost zero when in a regressing mode the pitch stirring frequency and the blade flapping frequency coincide. The wake amplitude reaches a maximum for a pitch stirring frequency somewhat below the blade

flapping natural frequency. For a collective pitch angle of 2° and blade flapping frequencies of P = 1.25 and 1.175 the test data were further evaluated by determining spanwise averages of $\bar{w}$, $|\overline{w^2}|^{1/2}$ and $|F_{1\omega}|_w$ that are proportional to the flapping moment of a blade at the hub.

The conclusion with respect to these hub moments are:

1. The hub moments from $\bar{w}$, $|\overline{w^2}|^{1/2}$ and $|F_{1\omega}|_w$ for 4 and 2 blades are not much different. This may not be true for higher collective pitch.
2. From comparing the blade flapping responses obtained analytically without dynamic wake and those obtained experimentally with the hub moments from the wake amplitude one can conclude that the large discrepancies between analytical and experimental blade flapping responses to steady cyclic pitch stirring must be primarily caused by the dynamic rotor wake.

Thirty transient pitch stirring tests at zero advance ratio have been conducted with 2°, 5°, 8° collective pitch. The testing time was less than one hour and only a fraction of what is required for frequency response tests. No conclusions can be drawn as to the test results since the data have not been processed as yet.

With respect to data handling systems, the only method feasible with presently available equipment is to digitize and preprocess the data on a PDP-12 computer and manually key punch cards for final processing with the main IBM-360 computer. Alternative systems may become available that would speed up data handling:

1. A larger core memory of the PDP-12 would allow to perform the entire data handling task on this computer.
2. An analog-digital converter unit compatible with the PDP-11 would avoid key punching since this computer has direct access to the main IBM 360.
3. An automatic key punch adapter for the PDP-12 computer would also avoid the manual transfer to IBM cards.

FIGURE CAPTIONS

Fig. 1	Velocity Probe Locations.
Figs. 2-5	Time average $\overline{w}$ of the wake velocity for 12 cyclic pitch stirring frequencies and for 7 radial stations for the 4 bladed rotor with first flapping frequency P = 1.17.
Figs. 6-9	Root mean square $(\overline{w^2})^{1/2}$ for 12 cyclic pitch stirring frequency and for 7 radial stations for the 4 bladed rotor, P = 1.17.
Figs. 10-13	Wake velocity amplitudes $\lvert F_{1\omega} \rvert_w$ for 12 cyclic pitch stirring frequencies and for 7 radial stations for the 4 bladed rotor, P = 1.17.
Figs. 11,12	Hub moments from $\overline{w}$ vs. cyclic pitch stirring frequency, 2 and 4 bladed rotor, P = 1.25 and 1.175.
Figs. 13,14	Hub moments from $\lvert F_{1\omega} \rvert_w$ vs. cyclic pitch stirring frequency, 2 and 4 bladed rotor, P = 1.25 and 1.175.
Figs. 15,16	Thrust deficiency from $\overline{w}$ vs. cyclic pitch stirring frequency, 2 and 4 bladed rotor, P = 1.25 and 1.175.
Figs. 17,18	Hub moments from $(\overline{w^2})^{1/2}$ vs. cyclic pitch stirring frequency, 2 and 4 bladed rotor, P = 1.25 and 1.175.
Figs. 19-22	Flapping response amplitude ratio and phase angle vs. cyclic pitch stirring frequency, 2 and 4 bladed rotor, P = 1.25 and 1.175.
Figs. 23,24	Difference in analytical and experimental flapping amplitudes compared with hub moment amplitude from dynamic wakes vs. cyclic pitch stirring frequency, 2 and 4 bladed rotor, P = 1.25 and 1.175.
Fig. 25	Rotor Head with Instrumentation.

Figure 1

Rotor Measurement Station Schmatic

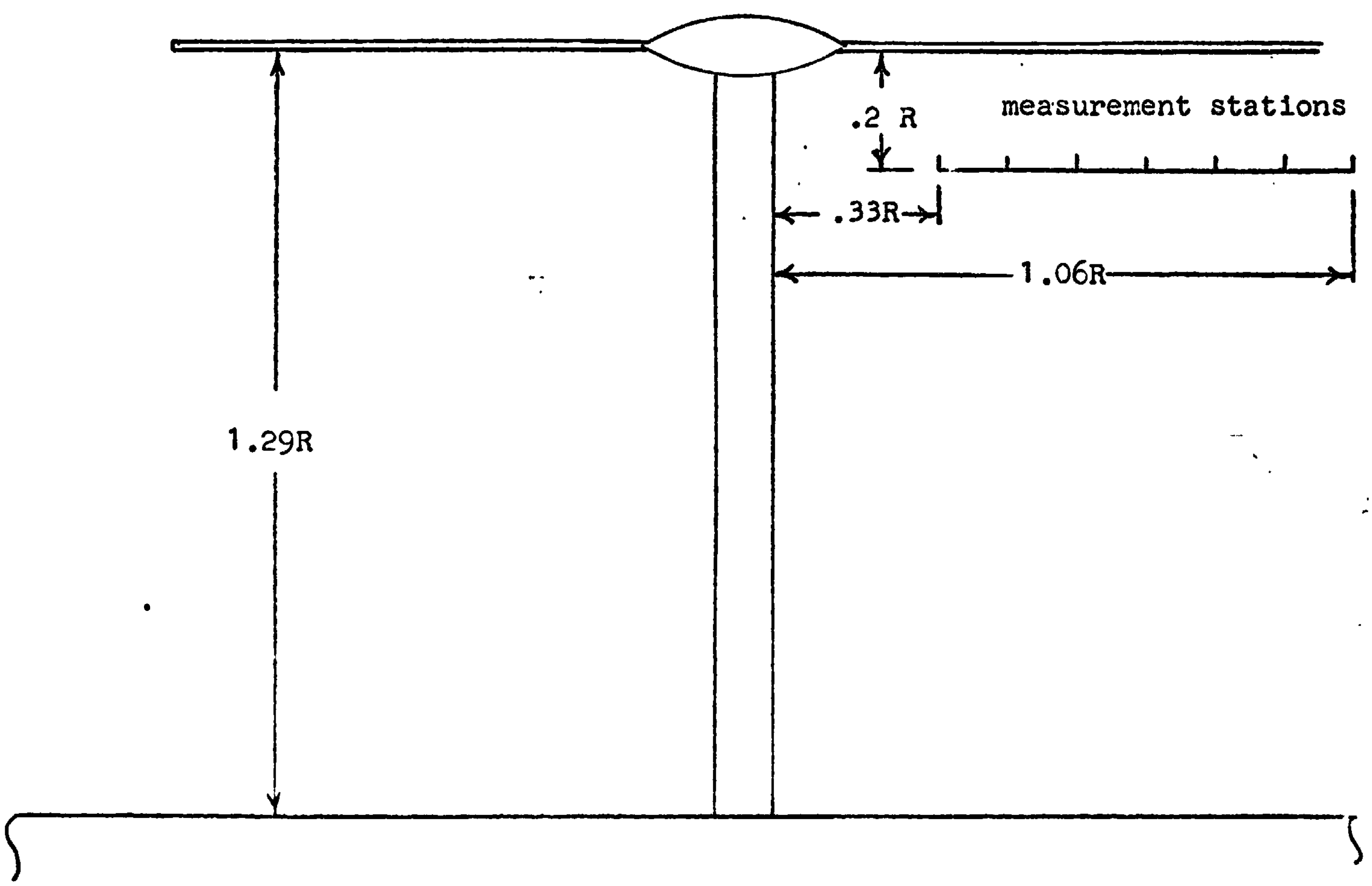

Figure 2a

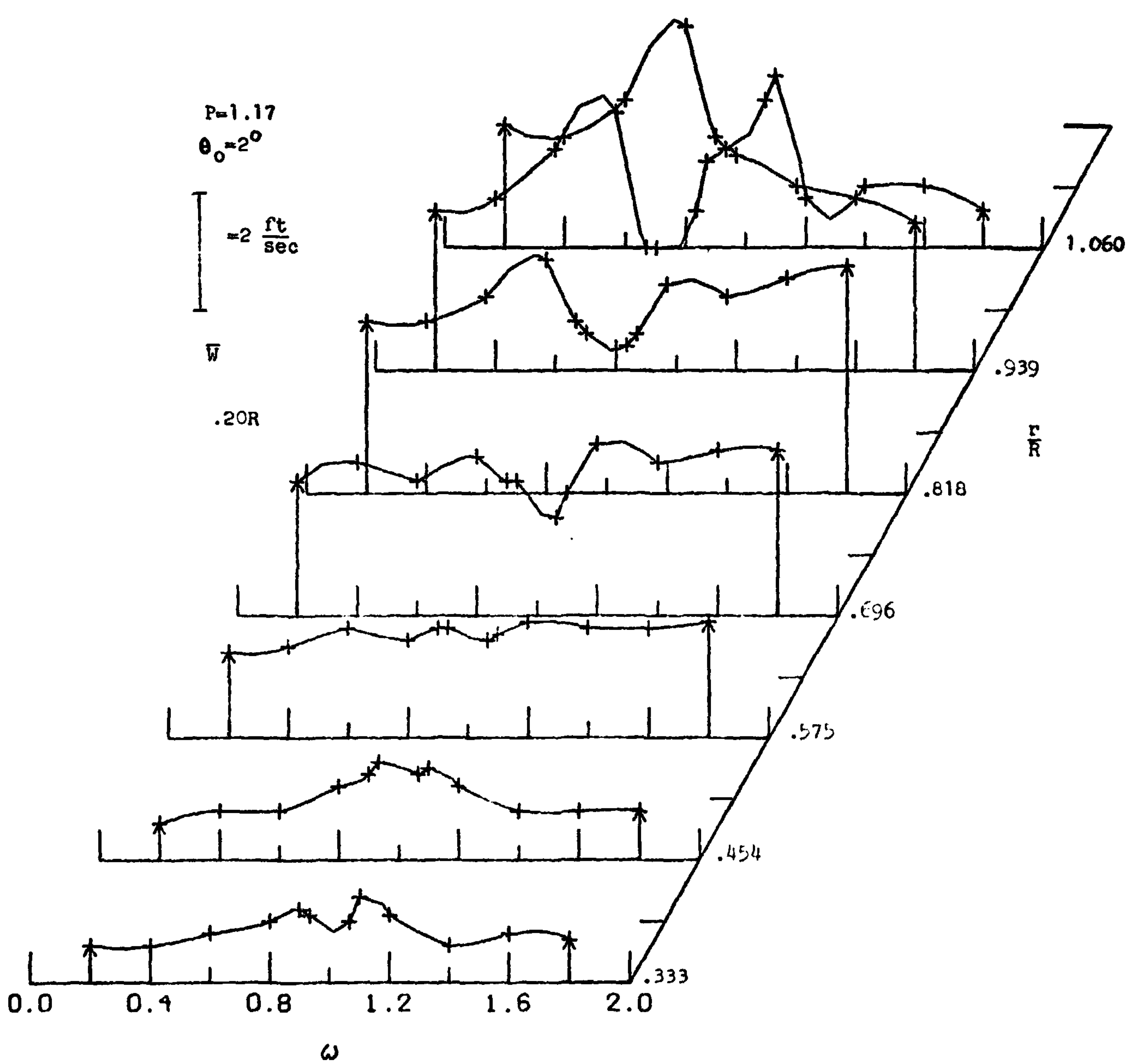
P=1.17
θ0=2°
=2 ft/sec
W̄
.20R
r/R
1.060
.939
.818
.696
.575
.454
.333
0.0
0.4
0.8
1.2
1.6
2.0
ω

Figure 2b

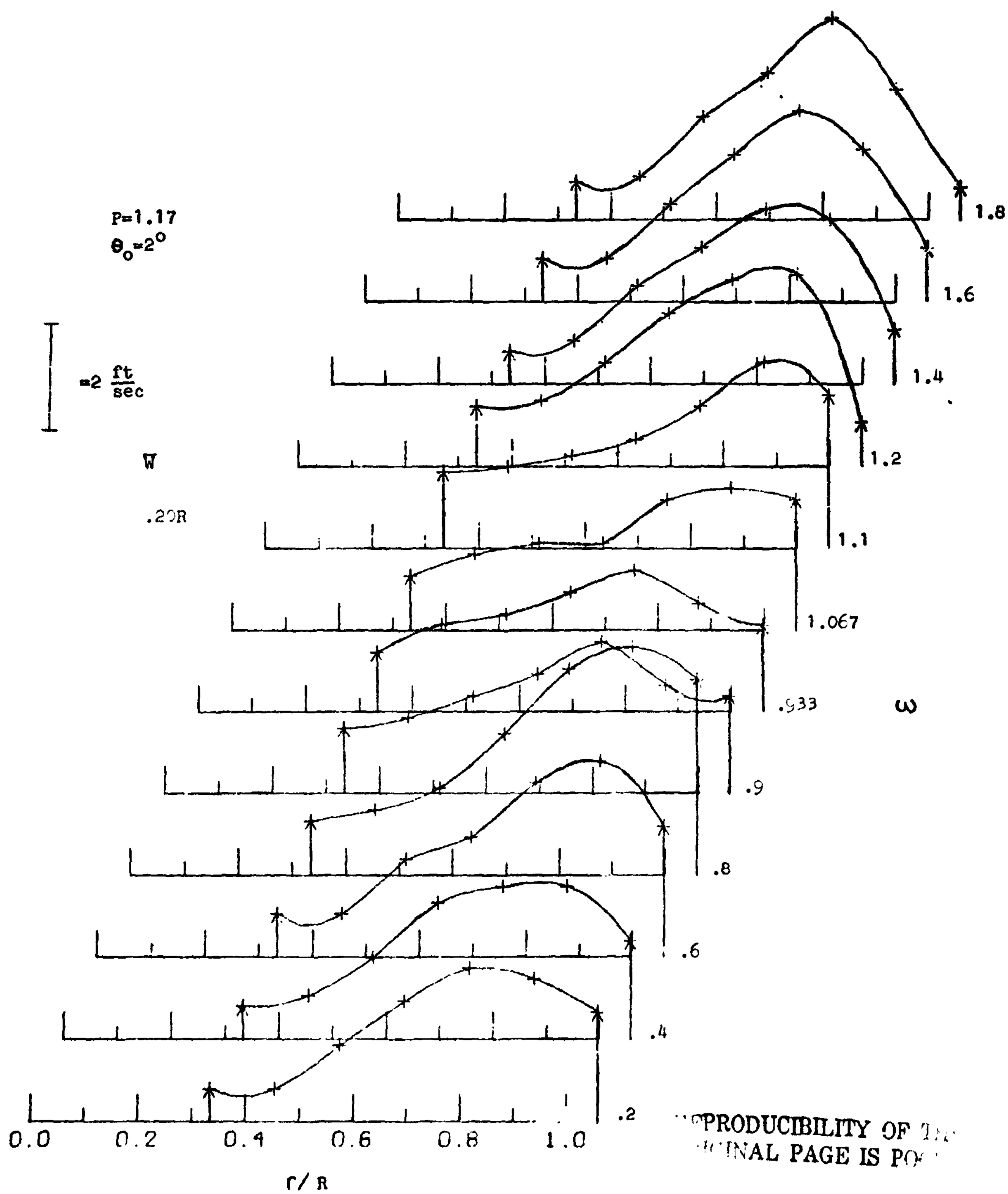
P=1.17
θ_o=2°
=2 ft/sec
W
.20R
1.8
1.6
1.4
1.2
1.1
1.067
.933
.9
.8
.6
.4
.2
ω
0.0
0.2
0.4
0.6
0.8
1.0
r/R

Figure 3a

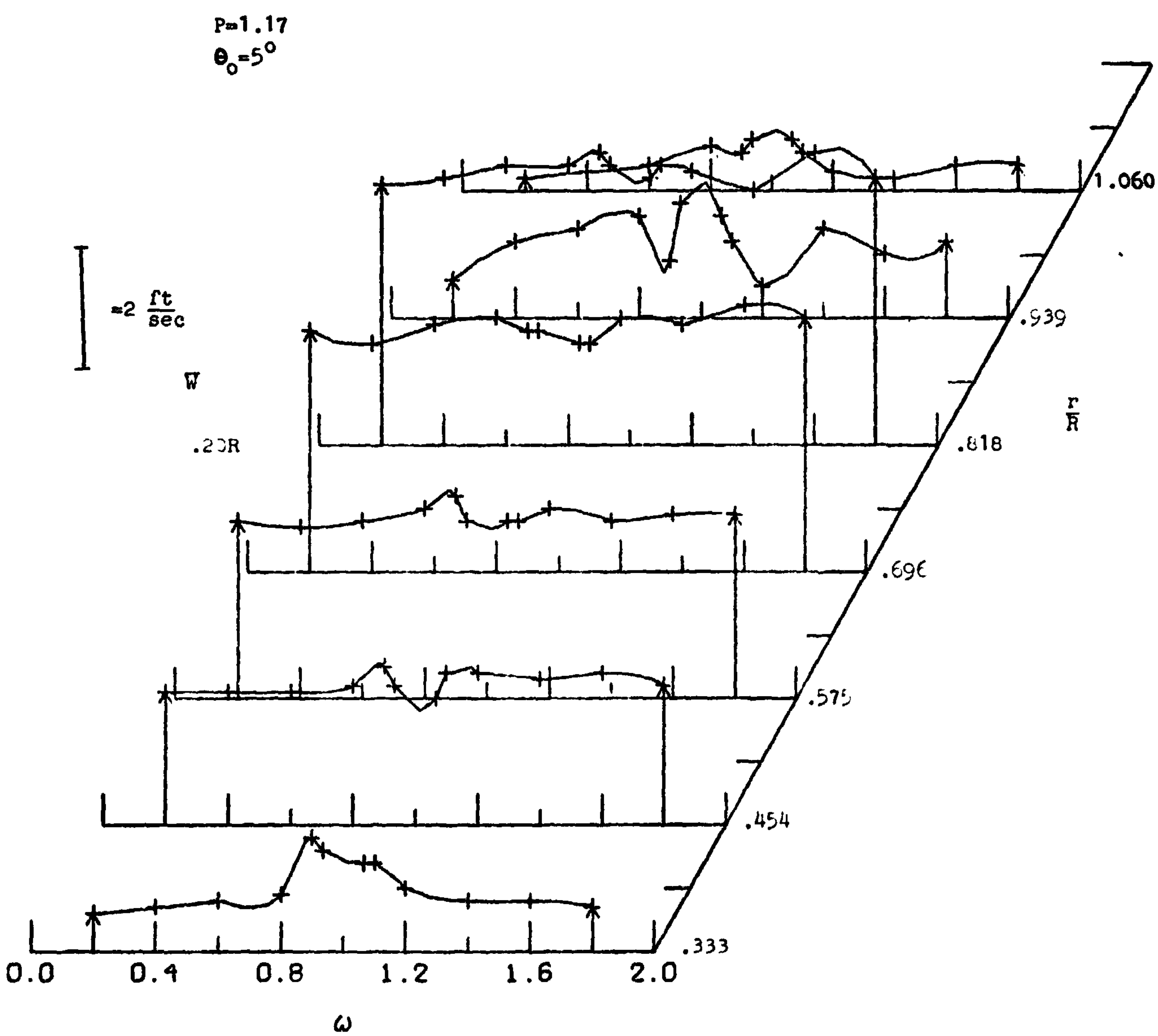
P=1.17
θ_0=5°
=2 ft/sec
W
.20R
r/R
1.060
.939
.818
.696
.575
.454
.333
0.0
0.4
0.8
1.2
1.6
2.0
ω

Figure 3b

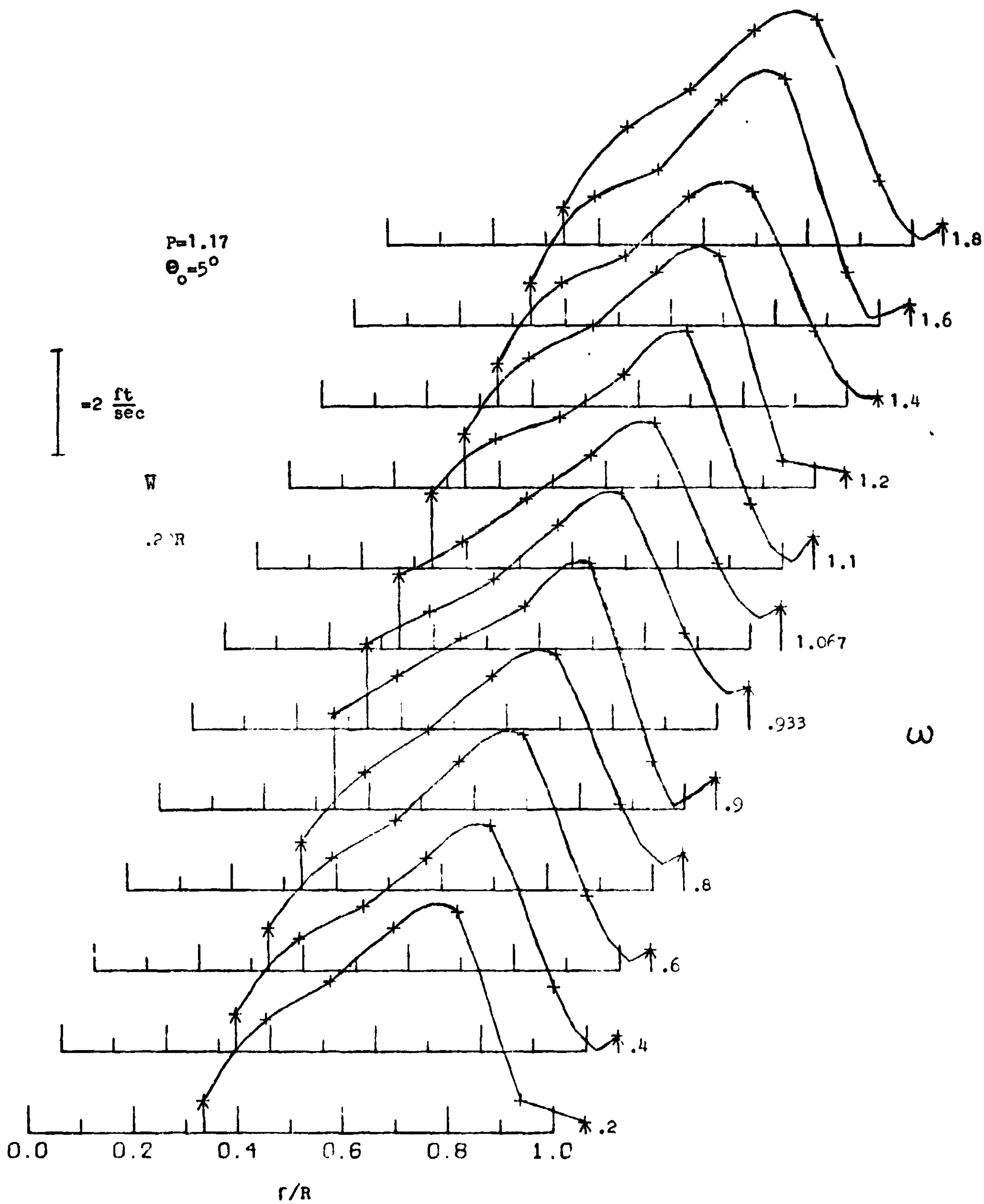
P=1.17
θ_o=5°
=2 ft/sec
W
.2 R
1.8
1.6
1.4
1.2
1.1
1.067
.933
.9
.8
.6
.4
.2
ω
0.0
0.2
0.4
0.6
0.8
1.0
r/R

Figure 4a

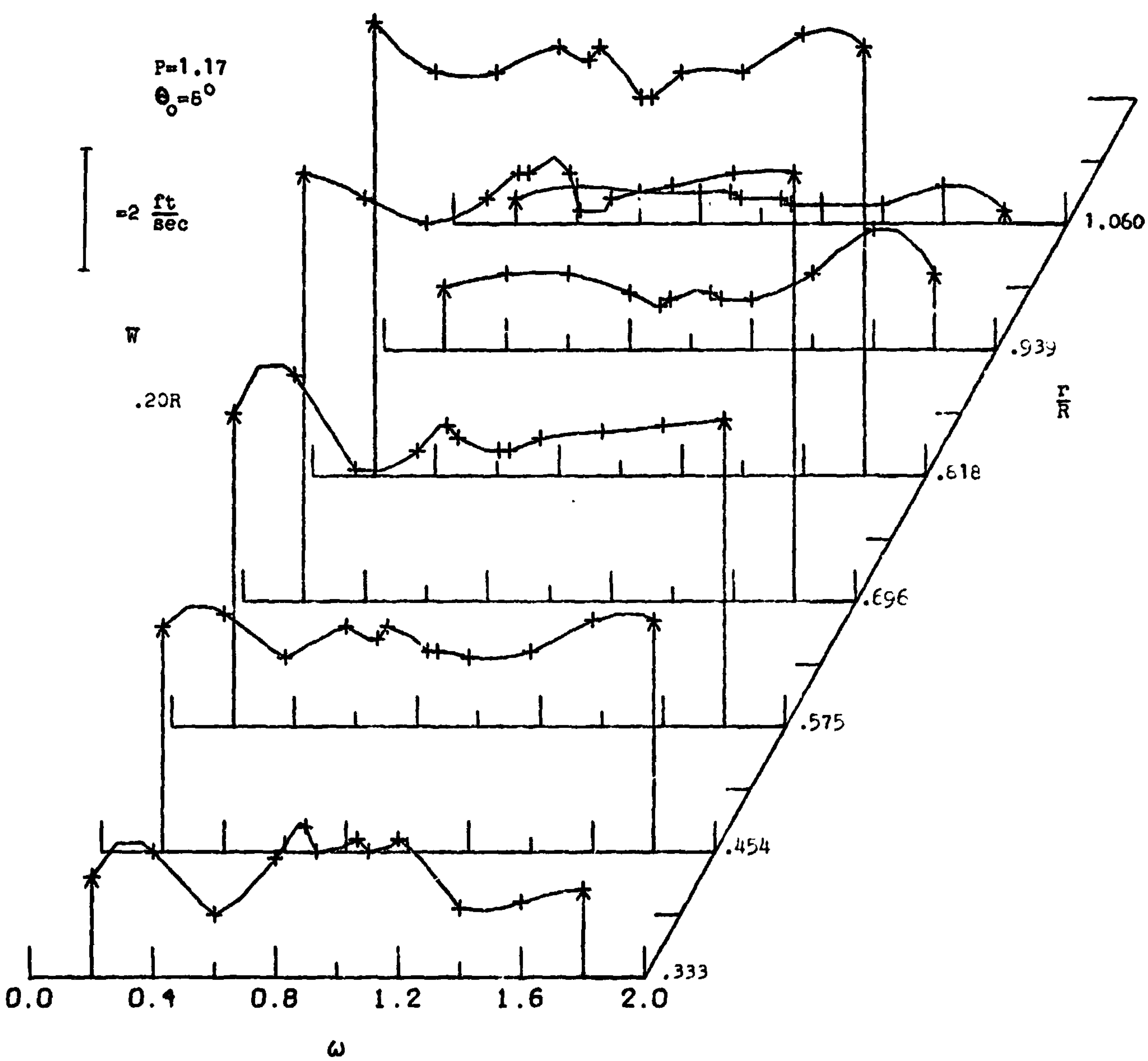
P=1.17
θ_o=6°
=2 ft/sec
W
.20R
1.060
.939
.818
.696
.575
.454
.333
r/R
0.0
0.4
0.8
1.2
1.6
2.0
ω

Figure 4b

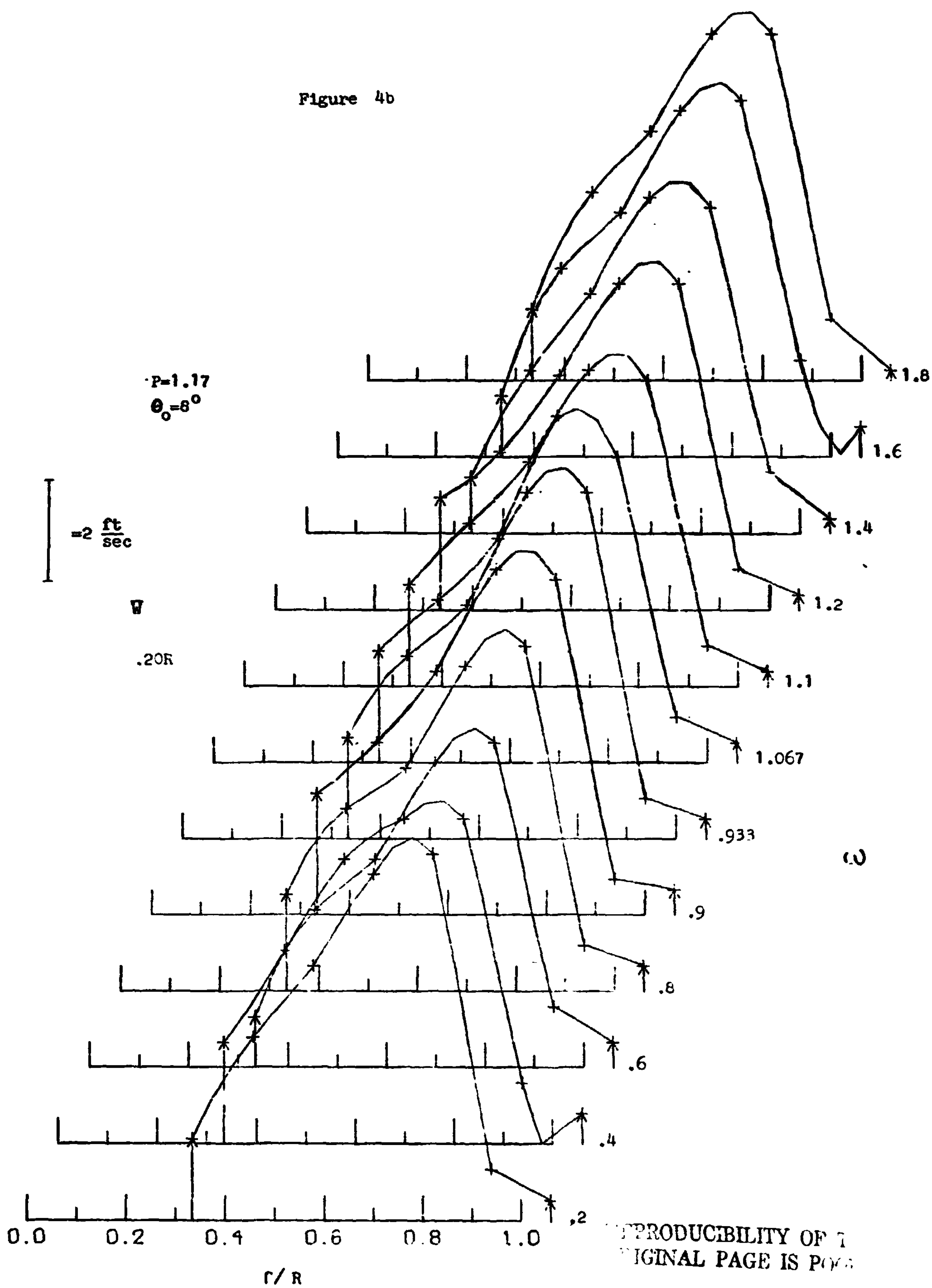
P=1.17
θ_0=8°
=2 ft/sec
W
.20R
1.8
1.6
1.4
1.2
1.1
1.067
.933
ω
.9
.8
.6
.4
,2
0.0
0.2
0.4
0.6
0.8
1.0
r/R

Figure 5a

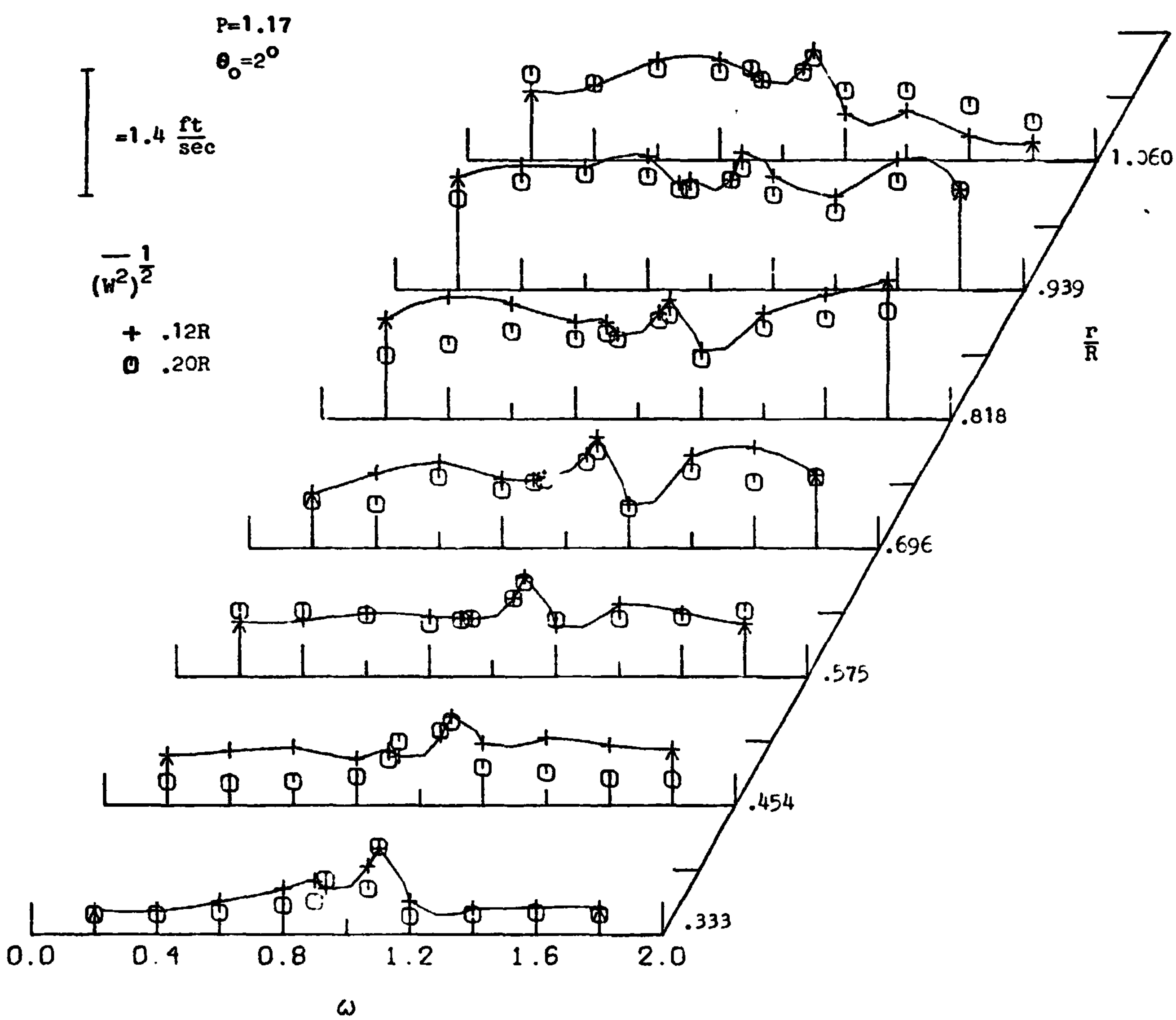
P=1.17
θ_o=2°
=1.4 ft/sec
$(\overline{W^2})^{\frac{1}{2}}$
+ .12R
O .20R
1.060
.939
.818
.696
.575
.454
.333
r/R
0.0
0.4
0.8
1.2
1.6
2.0
ω

Figure 5b

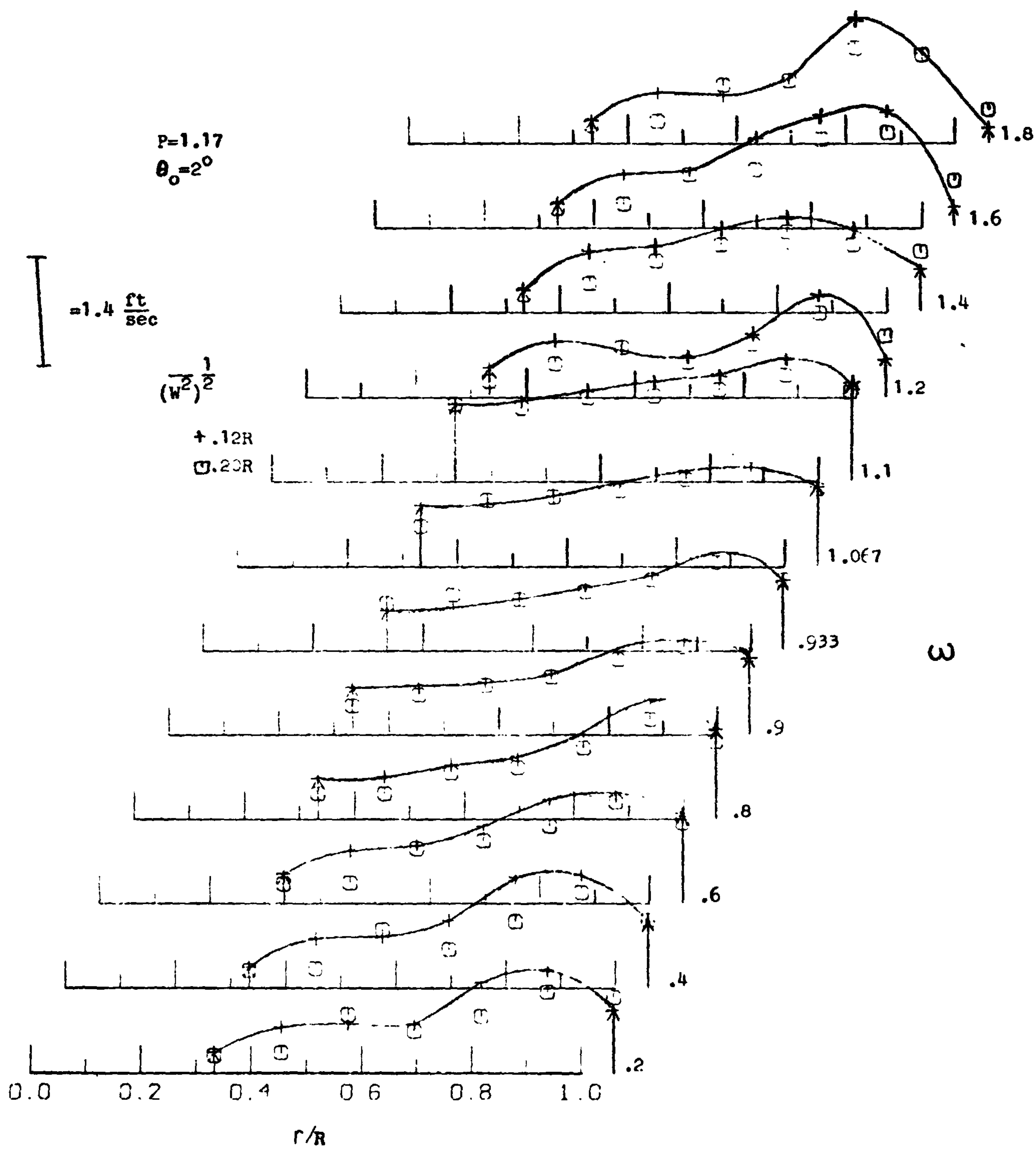
P=1.17
θ_o=2°
=1.4 ft/sec
$(\overline{W^2})^{\frac{1}{2}}$
+ .12R
.20R
1.8
1.6
1.4
1.2
1.1
1.067
.933
.9
.8
.6
.4
.2
ω
0.0
0.2
0.4
0.6
0.8
1.0
r/R

Figure 6a

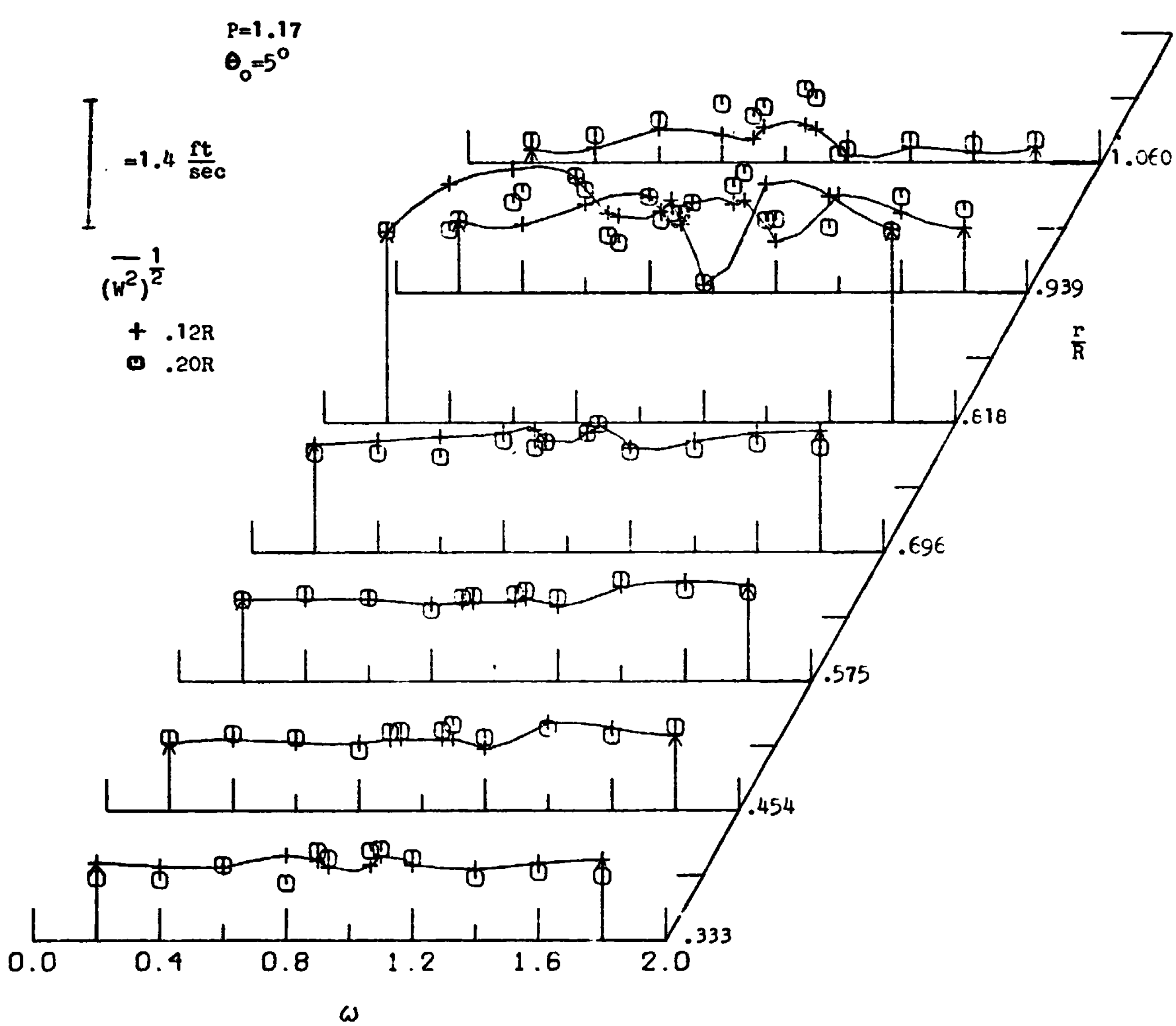
P=1.17
θ_o=5°
=1.4 ft/sec
$\overline{(W^2)}^{\frac{1}{2}}$
+ .12R
□ .20R
1.060
.939
.818
.696
.575
.454
.333
r/R
0.0
0.4
0.8
1.2
1.6
2.0
ω

Figure :b

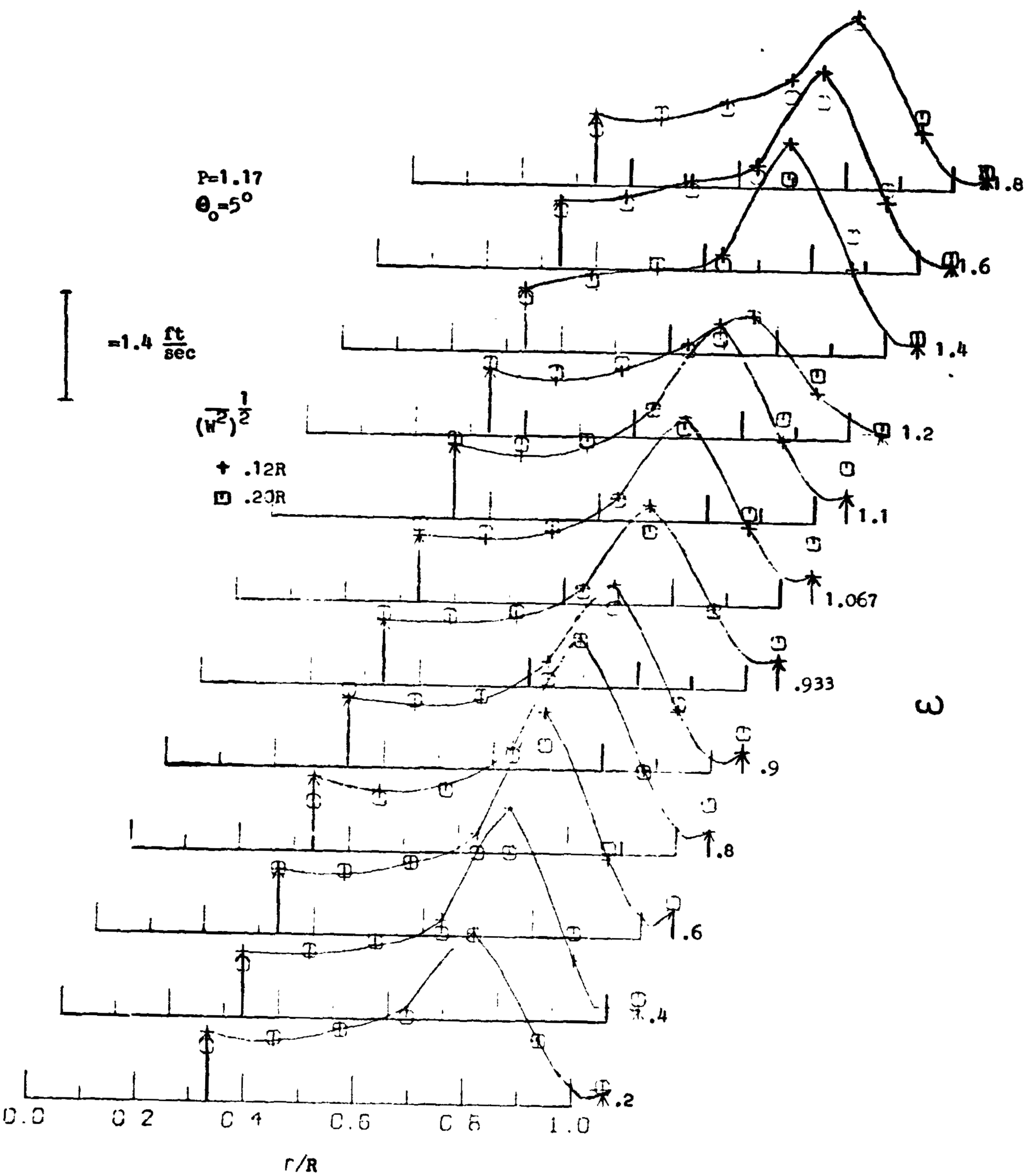
P=1.17
θ_o=5°
=1.4 ft/sec
$(\overline{W^2})^{\frac{1}{2}}$
+ .12R
⊡ .20R
1.8
1.6
1.4
1.2
1.1
1.067
.933
.9
.8
.6
.4
.2
ω
0.0
0.2
0.4
0.6
0.8
1.0
r/R

Figure 7a

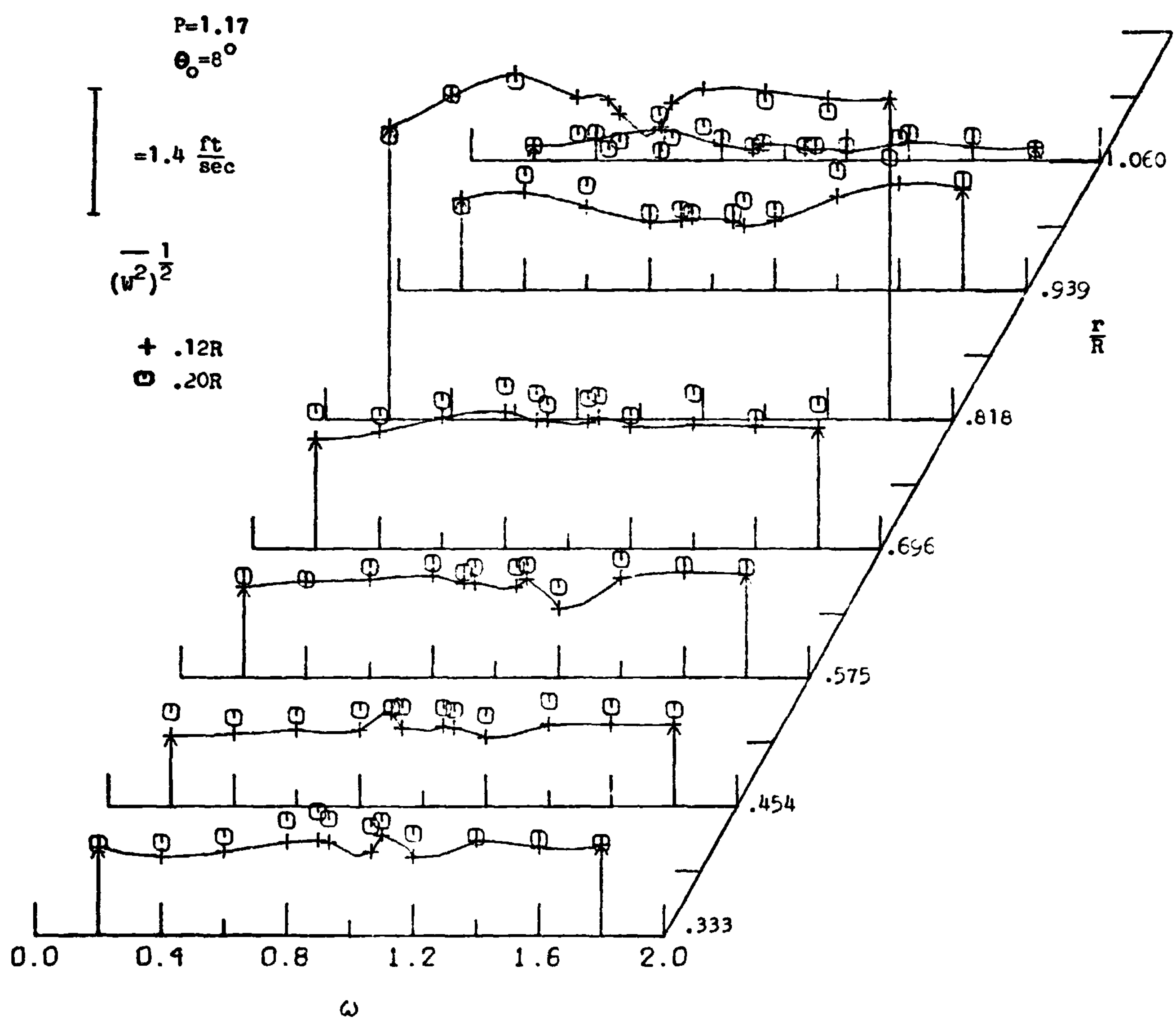
P=1.17
Θ_o=8°
=1.4 ft/sec
$(\overline{W^2})^{\frac{1}{2}}$
+ .12R
▫ .20R
1.060
.939
.818
.696
.575
.454
.333
r/R
0.0
0.4
0.8
1.2
1.6
2.0
ω

Figure 7b

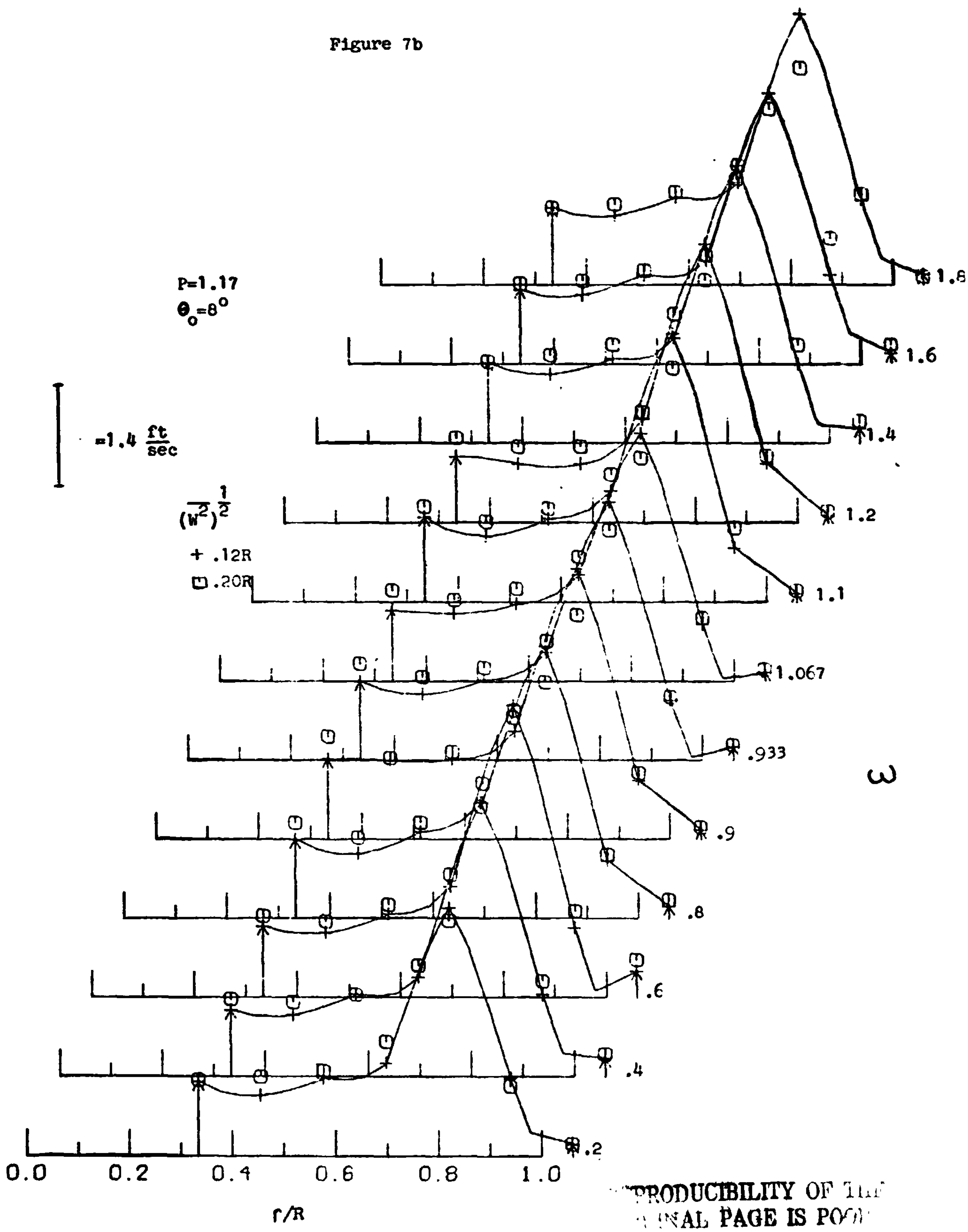
P=1.17
θ_o=8°
=1.4 ft/sec
$(\overline{W^2})^{\frac{1}{2}}$
+ .12R
.20R
1.8
1.6
1.4
1.2
1.1
1.067
.933
.9
.8
.6
.4
.2
0.0
0.2
0.4
0.6
0.8
1.0
r/R

3

Figure 8a

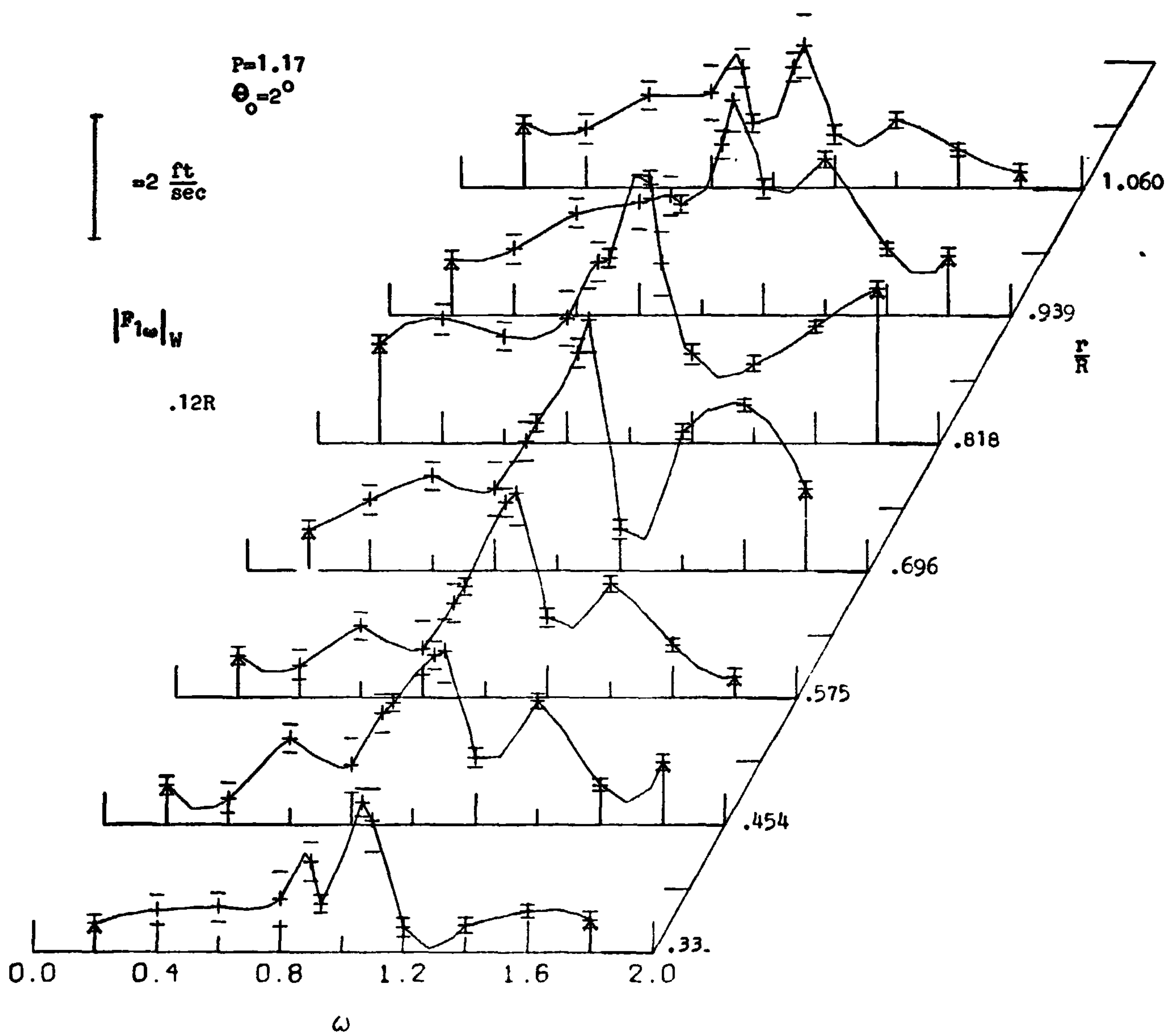
P=1.17
θ_o=2°
=2 ft/sec
$|F_{1\omega}|_W$
.12R
1.060
.939
.818
.696
.575
.454
.33
r/R
0.0
0.4
0.8
1.2
1.6
2.0
ω

Figure 8b

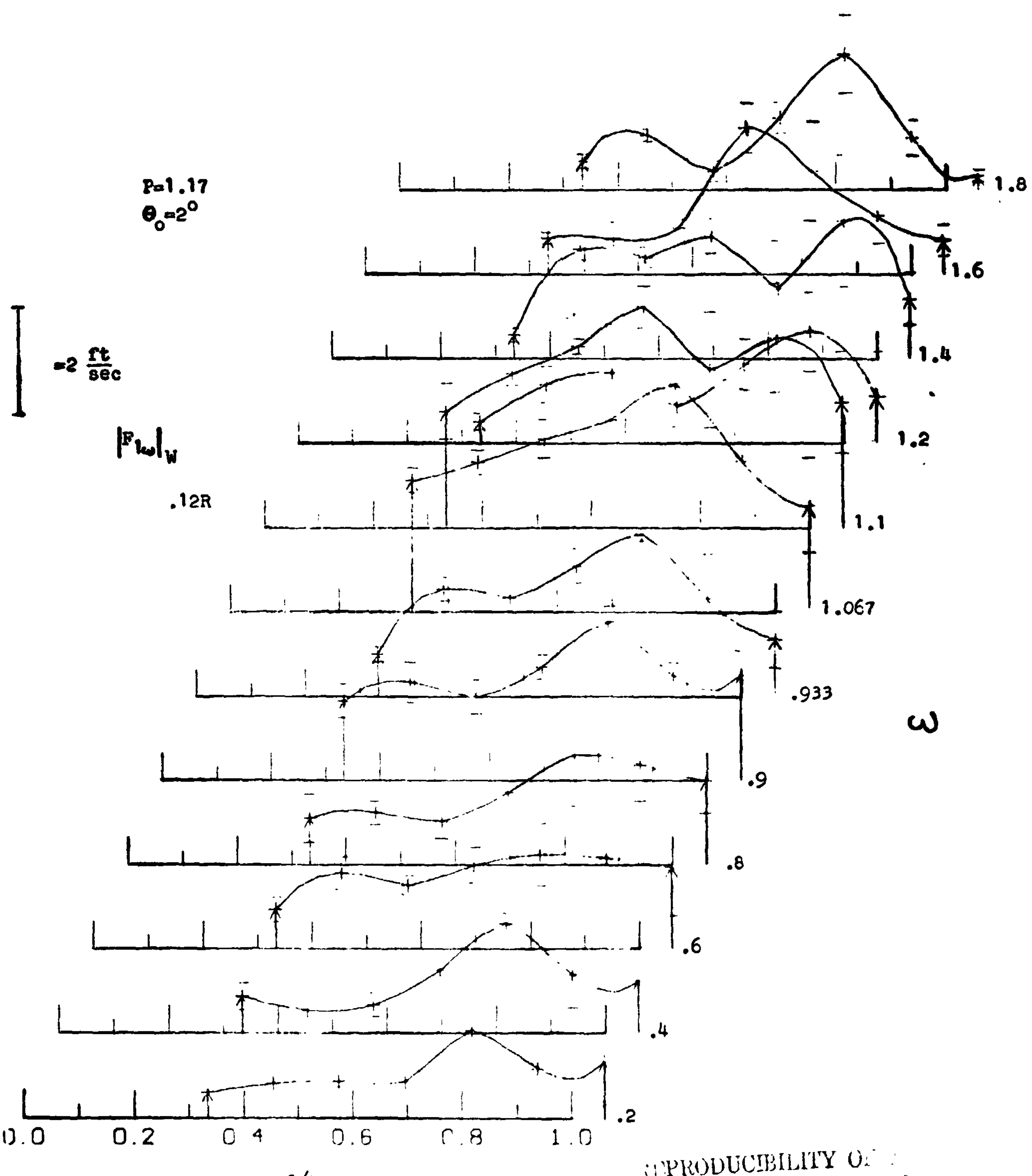
P=1.17
θ_o=2°
=2 $\frac{ft}{sec}$
$|F_{1\omega}|_W$
.12R
1.8
1.6
1.4
1.2
1.1
1.067
.933
.9
.8
.6
.4
.2
ω
0.0
0.2
0.4
0.6
0.8
1.0
r/R

Figure 9a

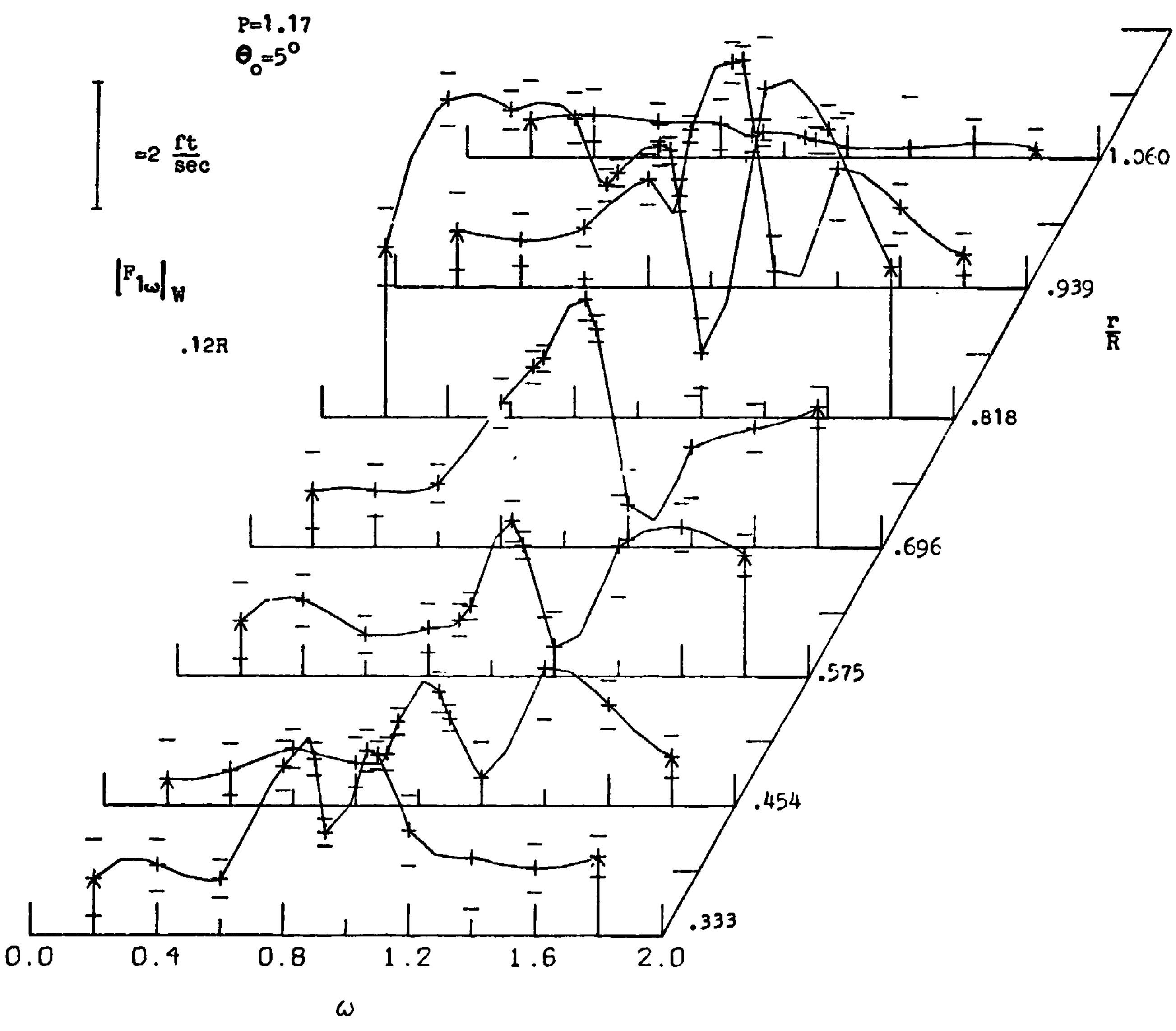
P=1.17
Θ_o=5°
=2 ft/sec
$|F_{1\omega}|_W$
.12R
1.060
.939
.818
.696
.575
.454
.333
r/R
0.0
0.4
0.8
1.2
1.6
2.0
ω

Figure 9b

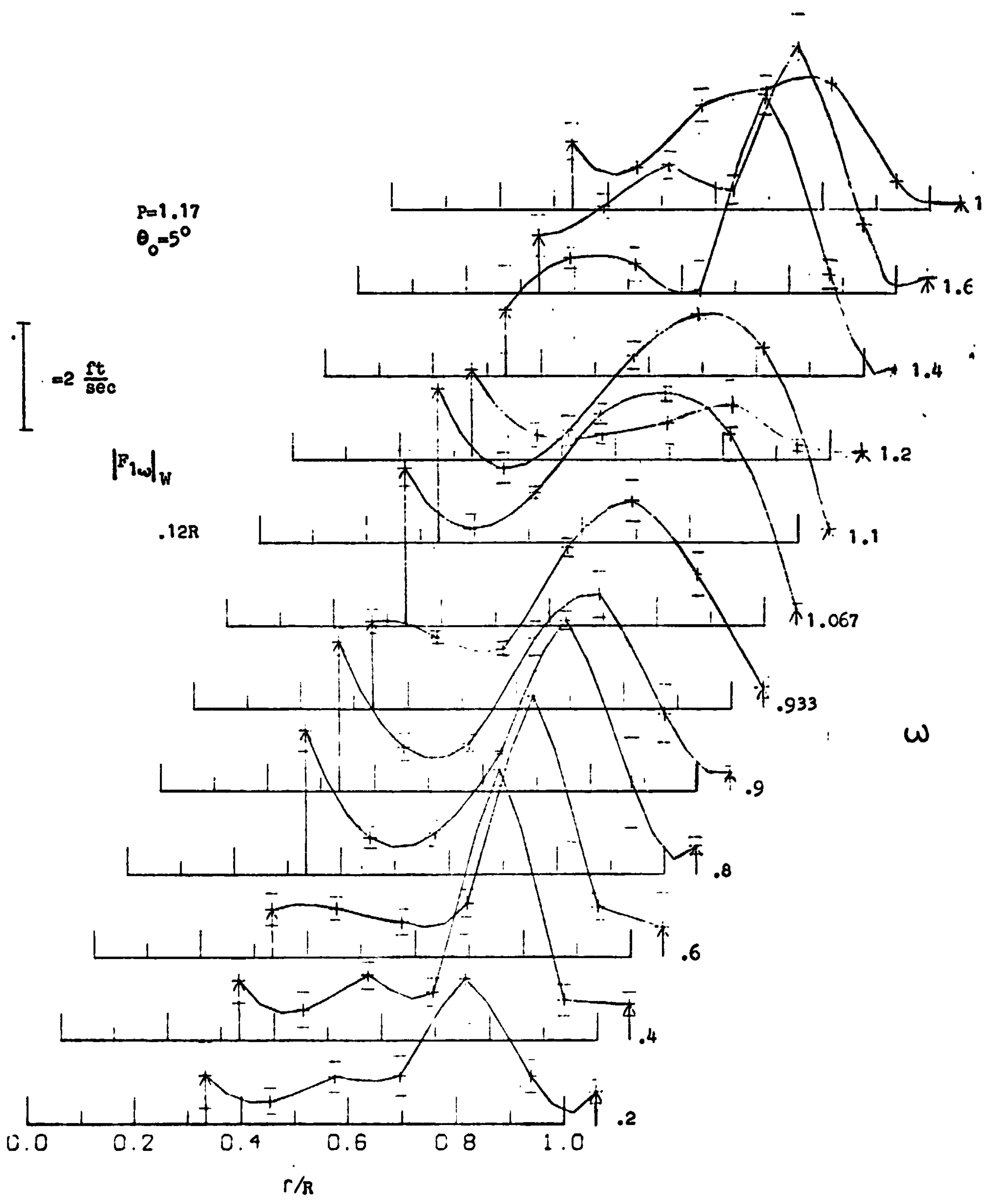
P=1.17
θ_o=5°
=2 ft/sec
$|F_{1\omega}|_W$
.12R
1.
1.6
1.4
1.2
1.1
1.067
.933
.9
.8
.6
.4
.2
ω
0.0
0.2
0.4
0.6
0.8
1.0
r/R

Figure 10a

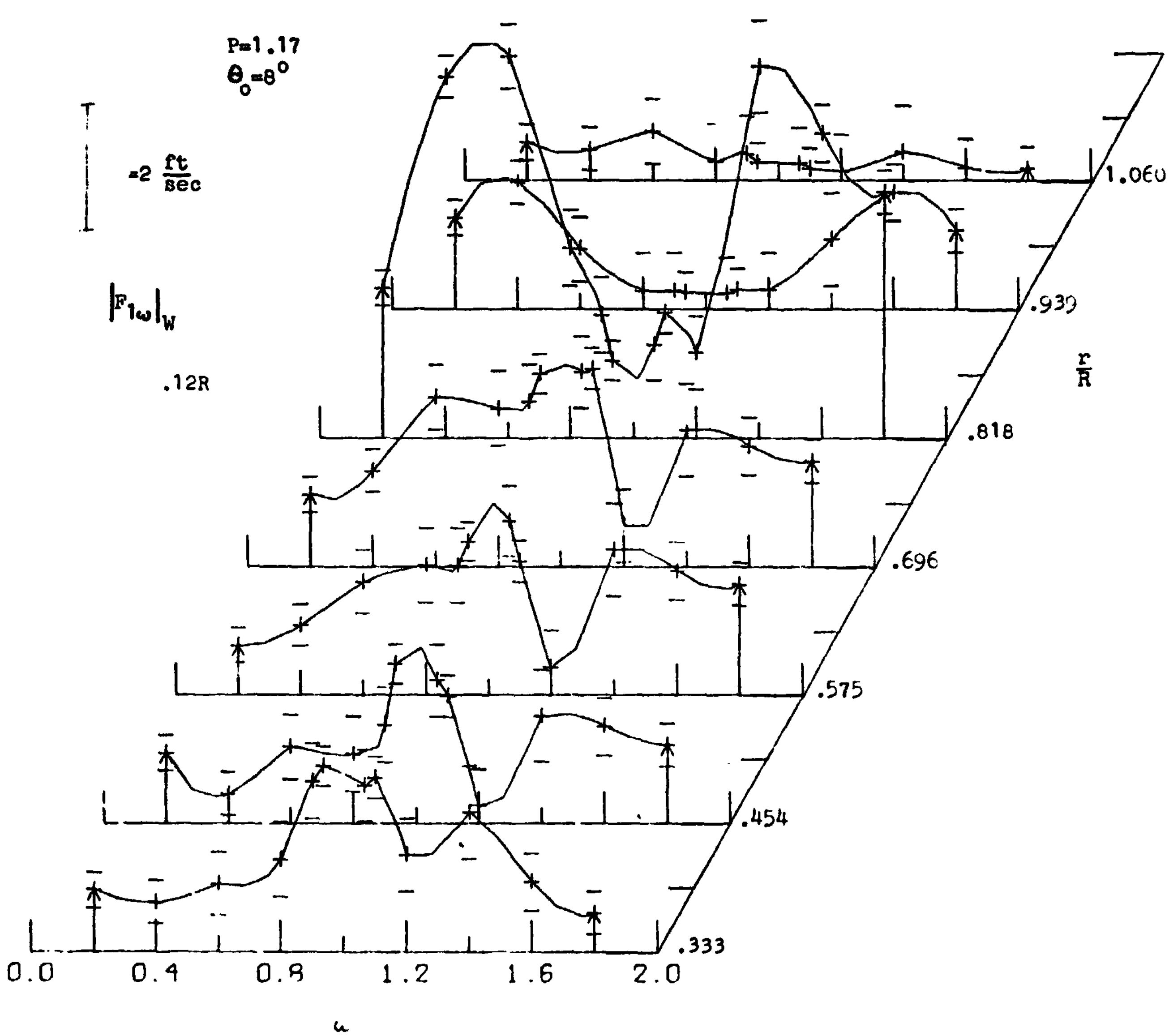
P=1.17
θ_o=8°
=2 ft/sec
$|F_{1\omega}|_W$
.12R
1.060
.939
.818
.696
.575
.454
.333
r/R
0.0
0.4
0.8
1.2
1.6
2.0
ω

Figure 10b

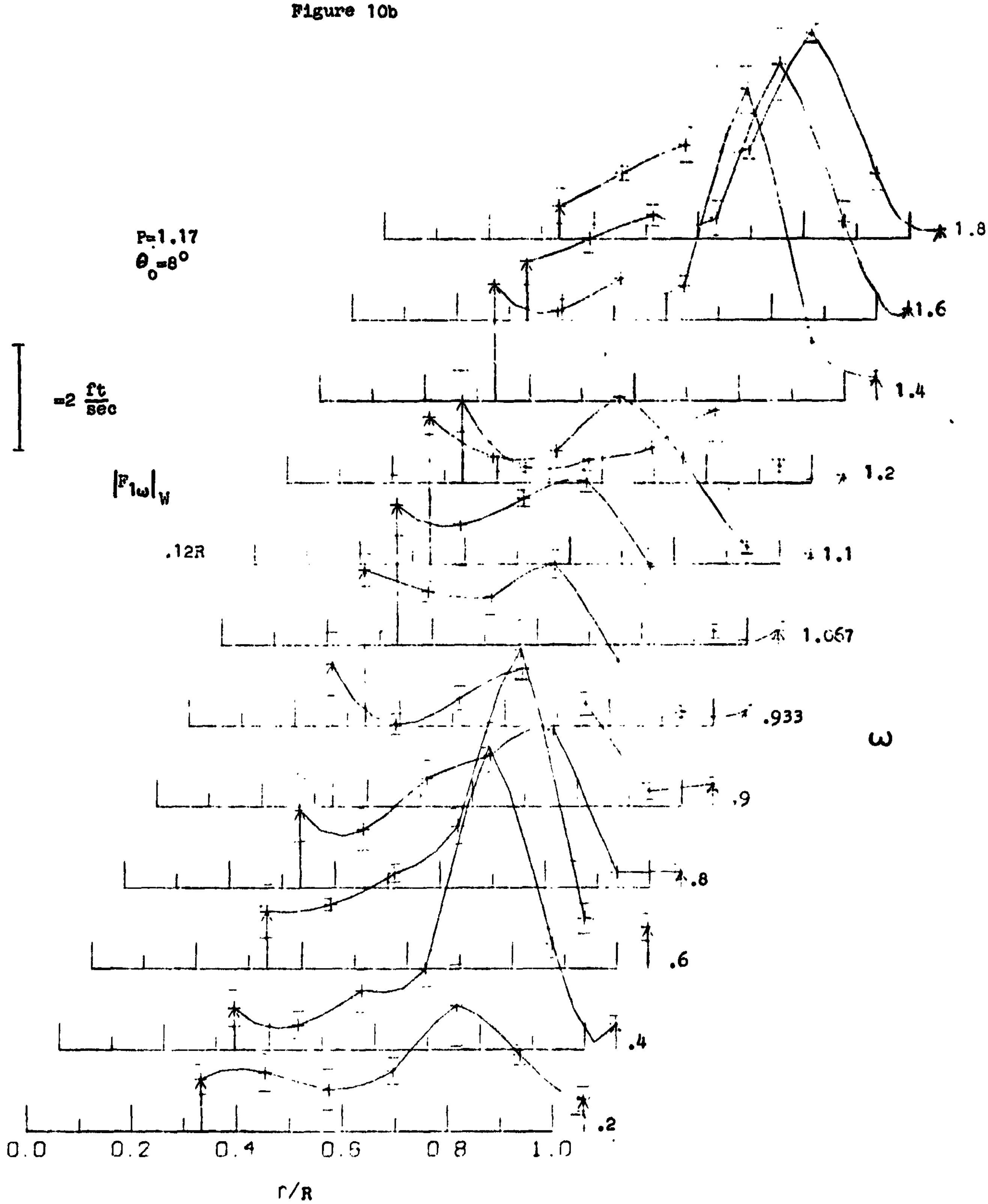
P=1.17
θ_o=8°
=2 ft/sec
$|F_{1\omega}|_W$
.12R
1.8
1.6
1.4
1.2
1.1
1.067
.933
ω
.9
.8
.6
.4
.2
0.0
0.2
0.4
0.6
0.8
1.0
r/R

Figure 11

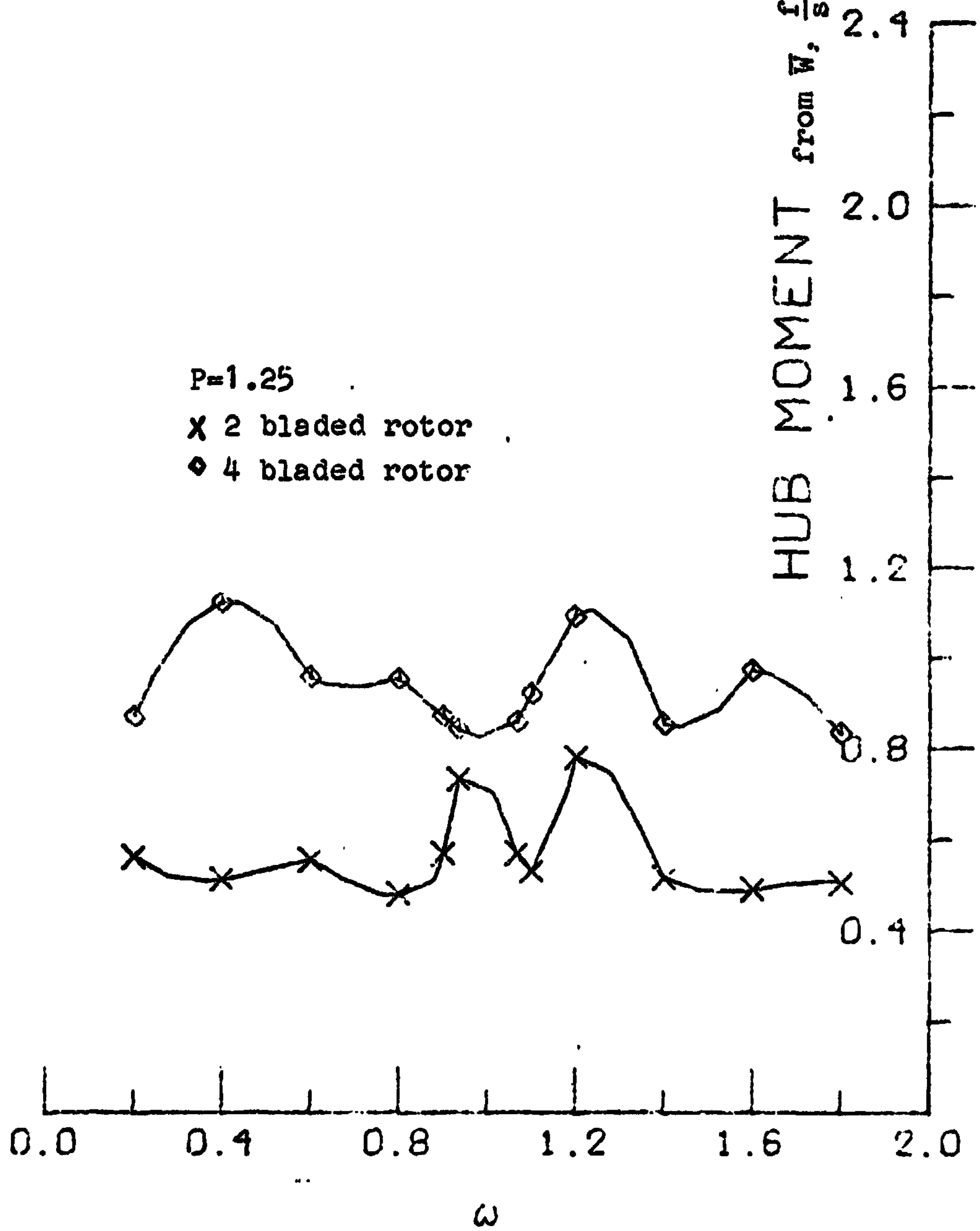
P=1.25
X 2 bladed rotor
◇ 4 bladed rotor
HUB MOMENT from W, ft/sec
2.4
2.0
1.6
1.2
0.8
0.4
0.0
0.4
0.8
1.2
1.6
2.0
ω

Figure 12

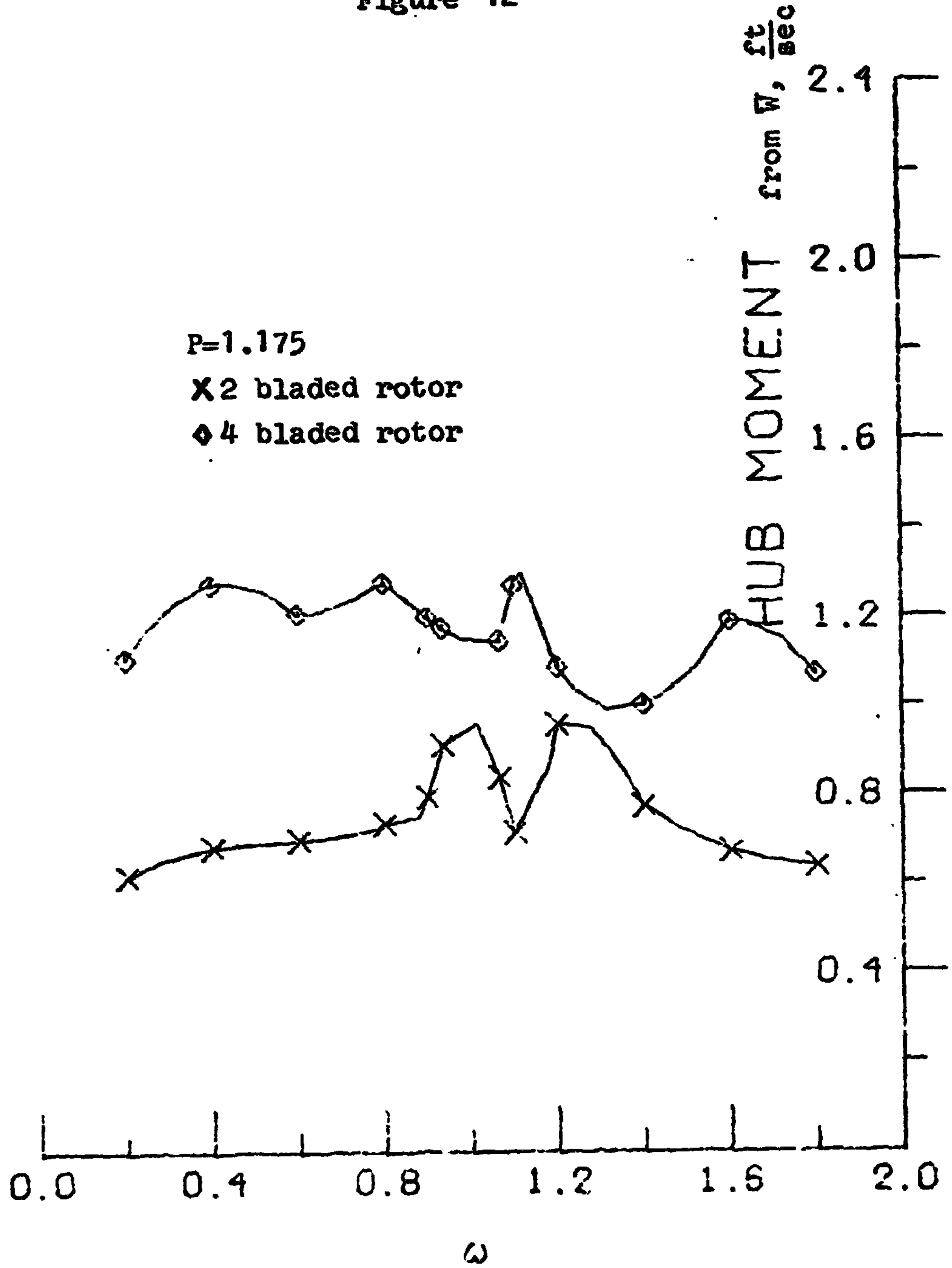
HUB MOMENT from W̄, ft/sec
2.4
2.0
1.6
1.2
0.8
0.4
P=1.175
X 2 bladed rotor
◆ 4 bladed rotor
0.0
0.4
0.8
1.2
1.6
2.0
ω

Figure 13

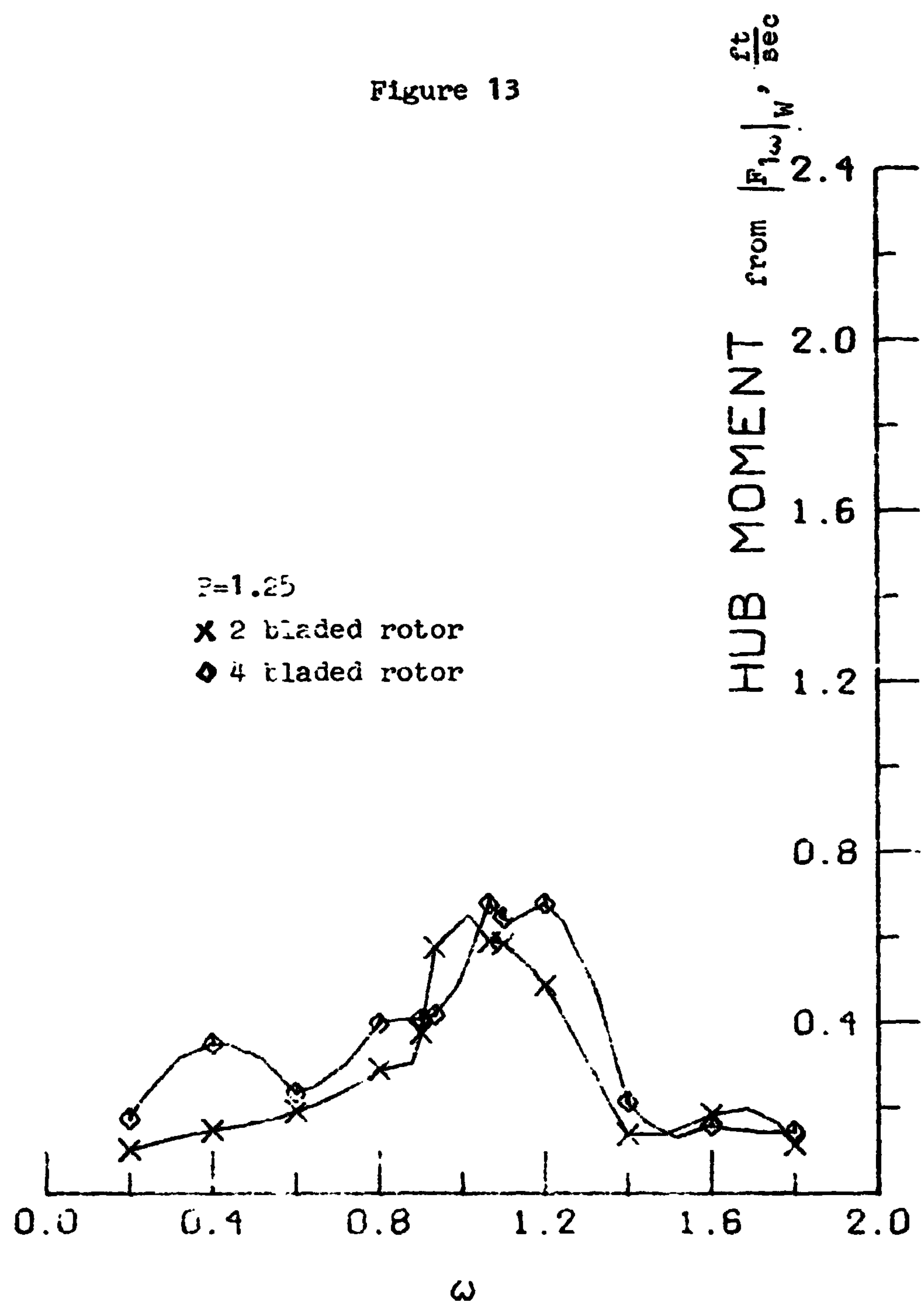
HUB MOMENT from $|F_{1\omega}|_W$, $\frac{ft}{sec}$
2.4
2.0
1.6
1.2
0.8
0.4
P=1.25
2 bladed rotor
4 bladed rotor
0.0
0.4
0.8
1.2
1.6
2.0
ω

Figure 14

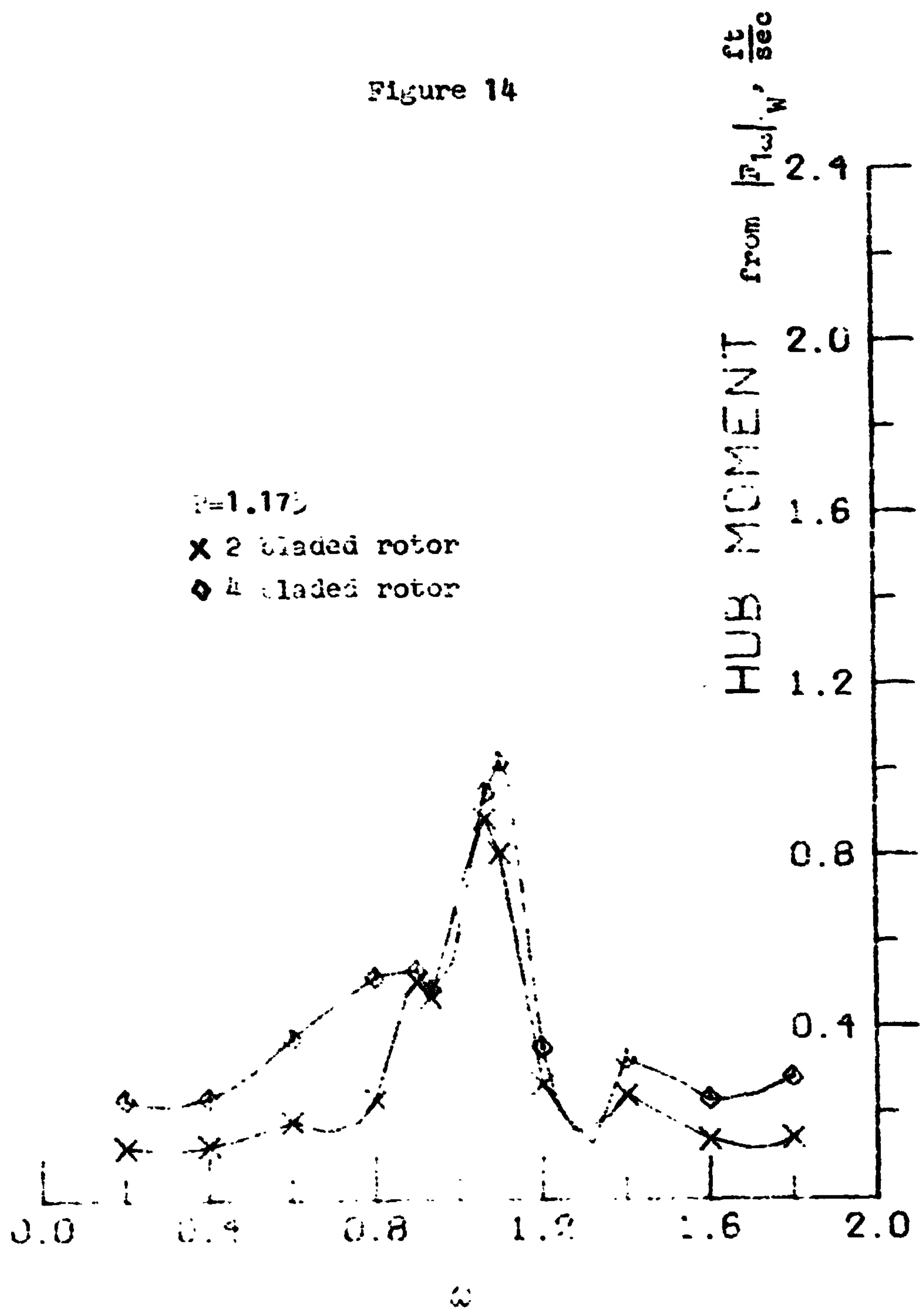

2 bladed rotor
4 bladed rotor
HUB MOMENT from $|F_{1\omega}|_w$, $\frac{ft}{sec}$
2.4
2.0
1.6
1.2
0.8
0.4
0.0
0.8
1.6
2.0
ω

Figure 15

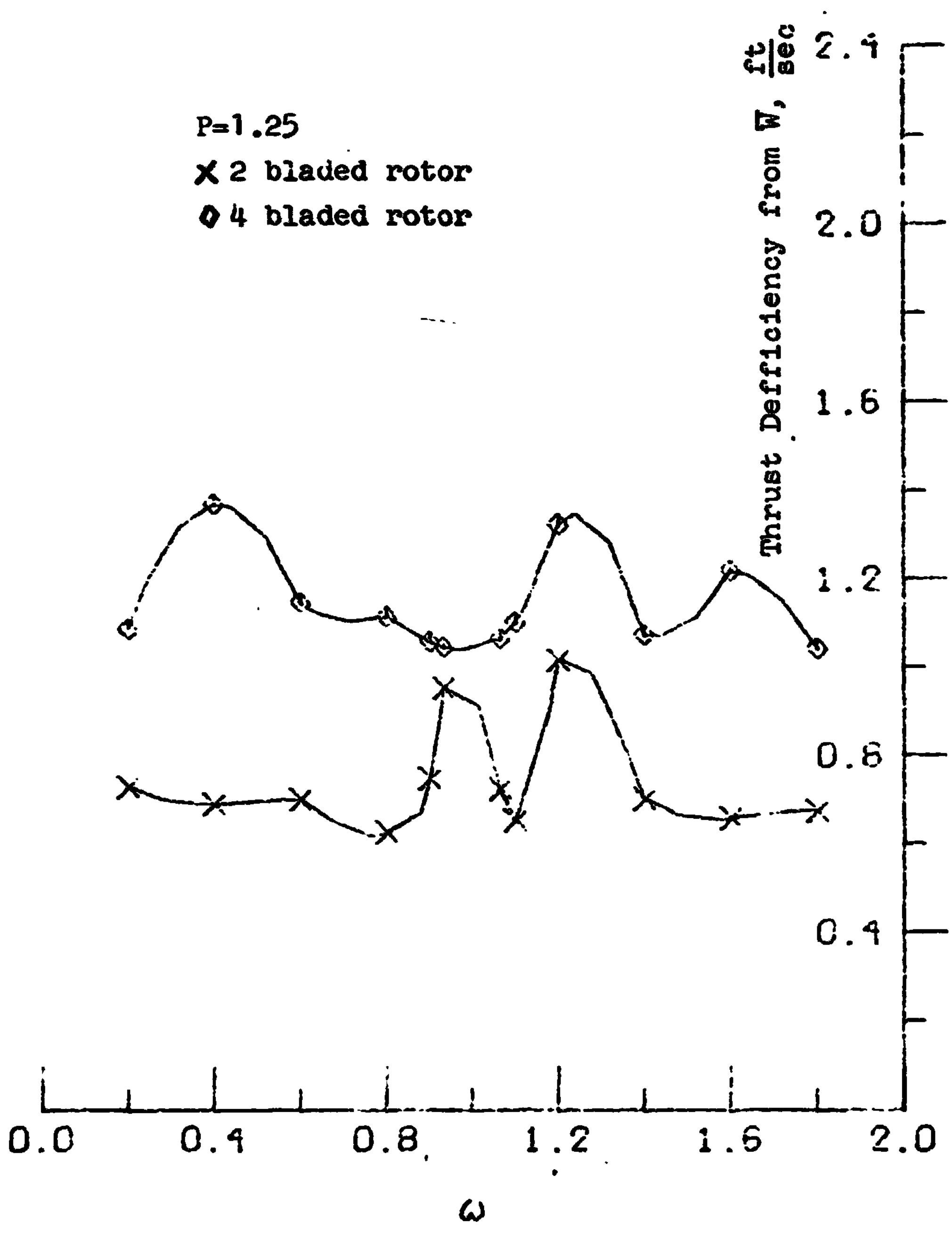
P=1.25
2 bladed rotor
4 bladed rotor
Thrust Defficiency from W, ft/sec
2.4
2.0
1.6
1.2
0.8
0.4
0.0
0.4
0.8
1.2
1.6
2.0
ω

Figure 16

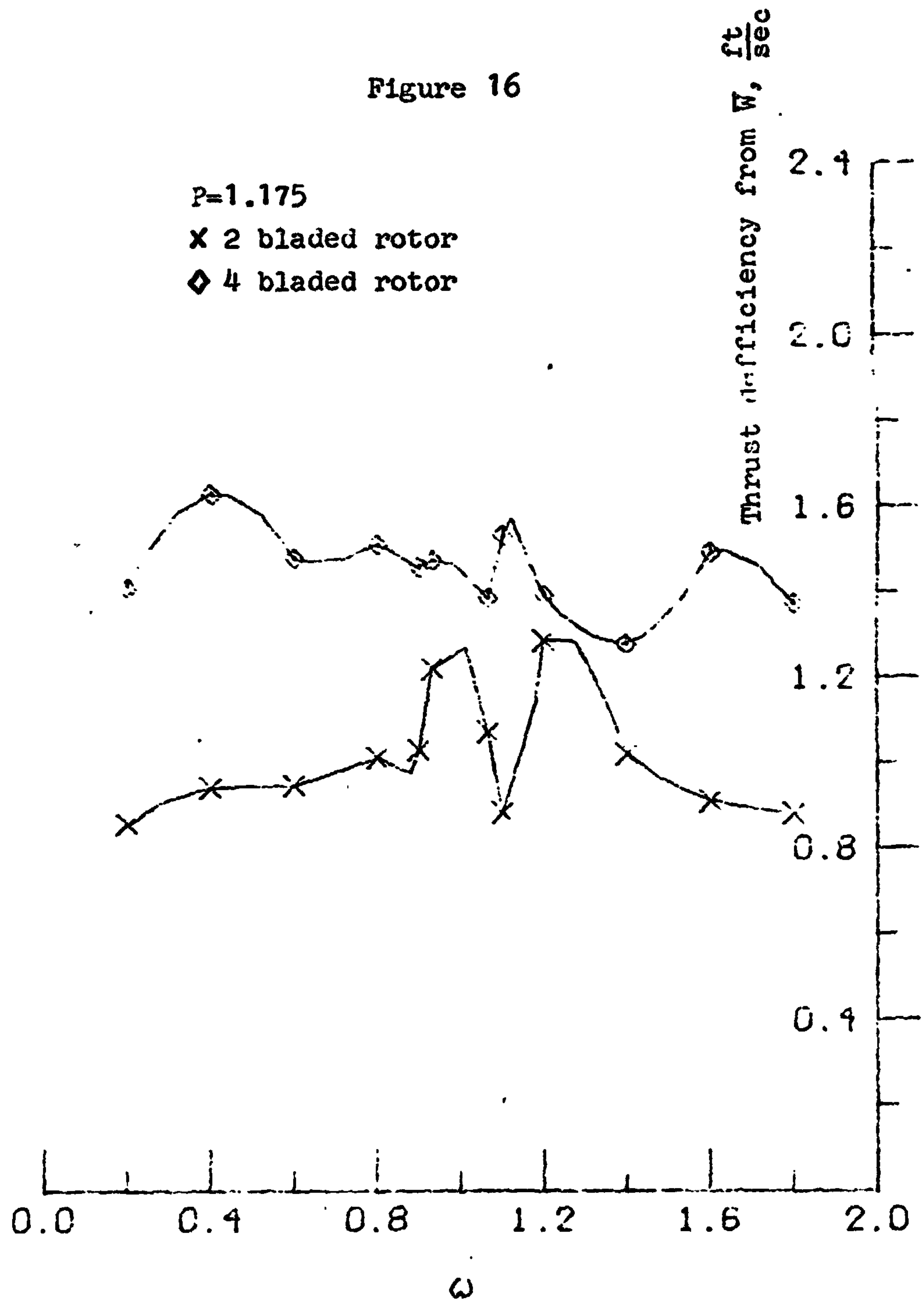
P=1.175
X 2 bladed rotor
◇ 4 bladed rotor
Thrust efficiency from W, ft/sec
2.4
2.0
1.6
1.2
0.8
0.4
0.0
0.4
0.8
1.2
1.6
2.0
ω

Figure 17

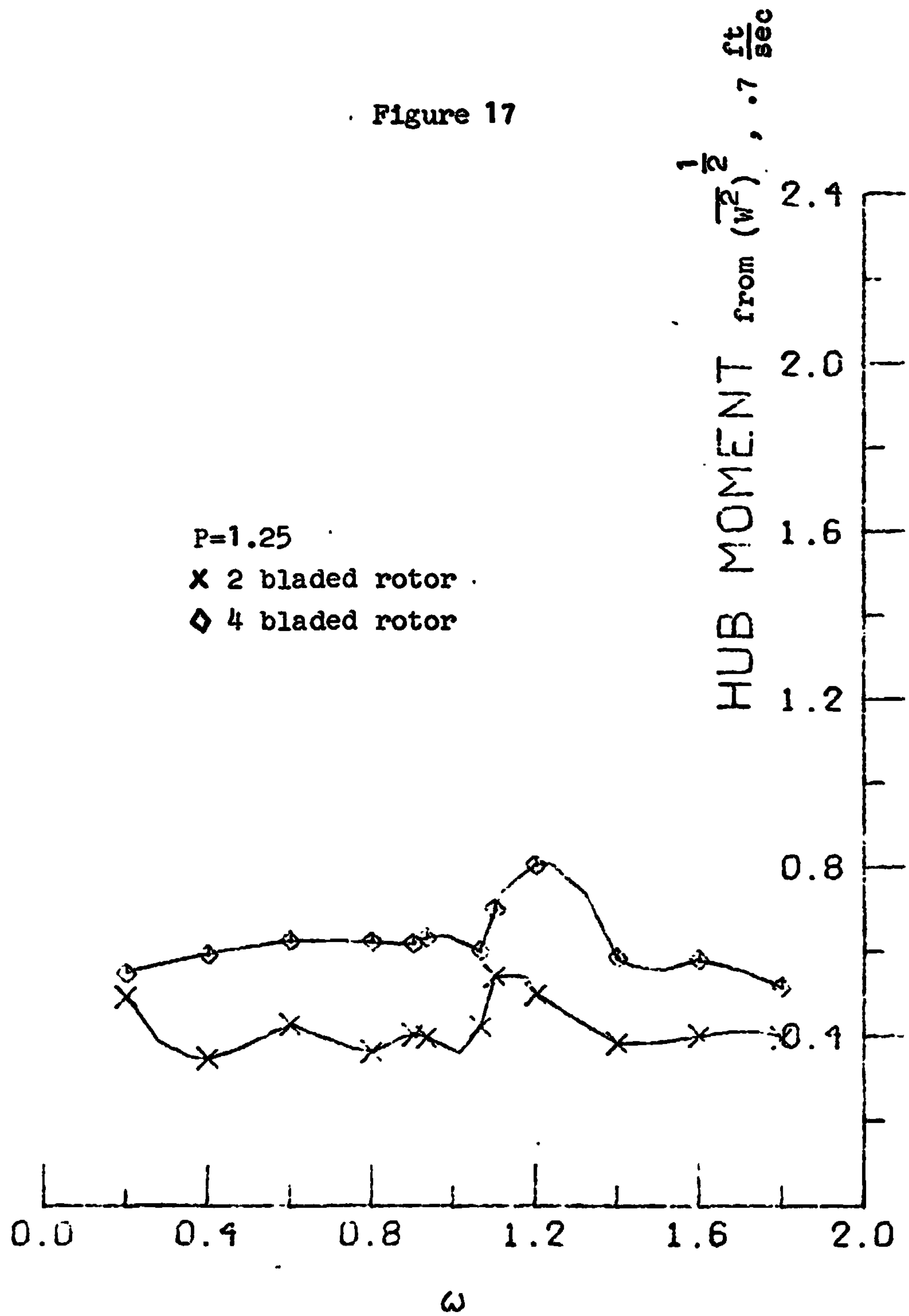
HUB MOMENT from $(\overline{w^2})^{\frac{1}{2}}$, .7 $\frac{ft}{sec}$
2.4
2.0
1.6
1.2
0.8
0.4
P=1.25
X 2 bladed rotor
◊ 4 bladed rotor
0.0
0.4
0.8
1.2
1.6
2.0
ω

Figure 18

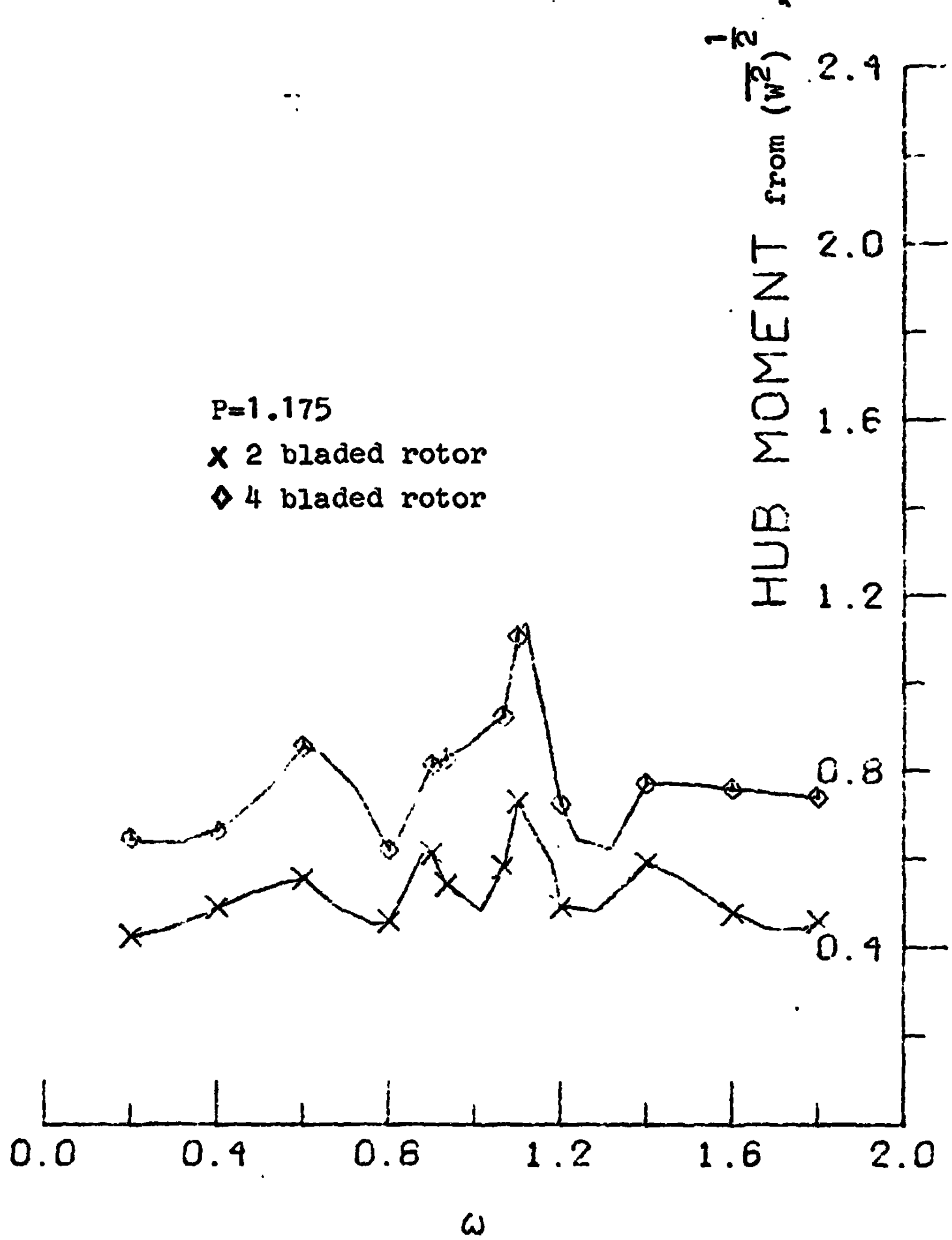

P=1.175
X 2 bladed rotor
◊ 4 bladed rotor
HUB MOMENT from $(\overline{w^2})^{1/2}$, .7 ft/sec
2.4
2.0
1.6
1.2
0.8
0.4
0.0
0.4
0.8
1.2
1.6
2.0
ω

Θ_0=2° μ=0.0

Figure 19

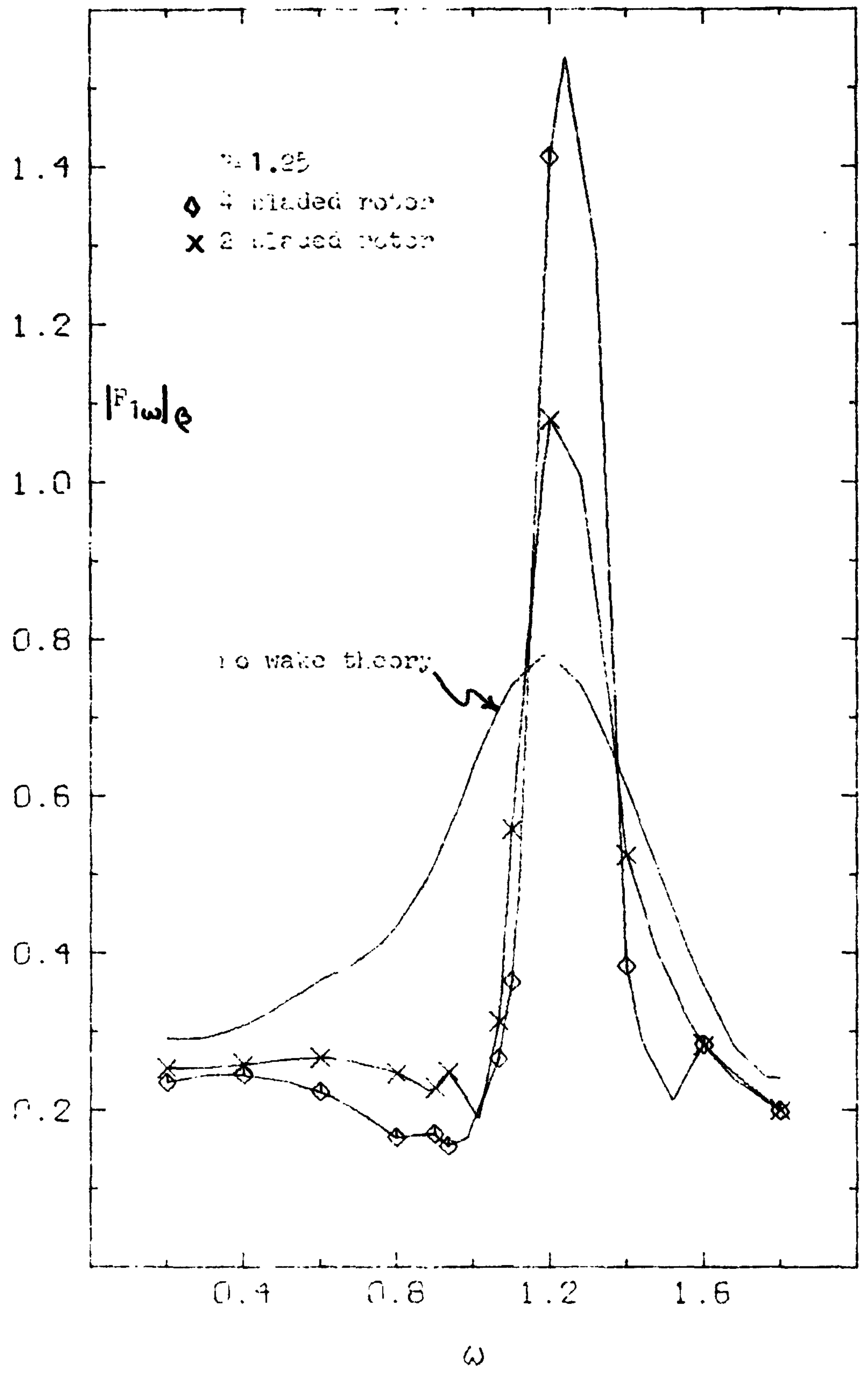

Figure 20

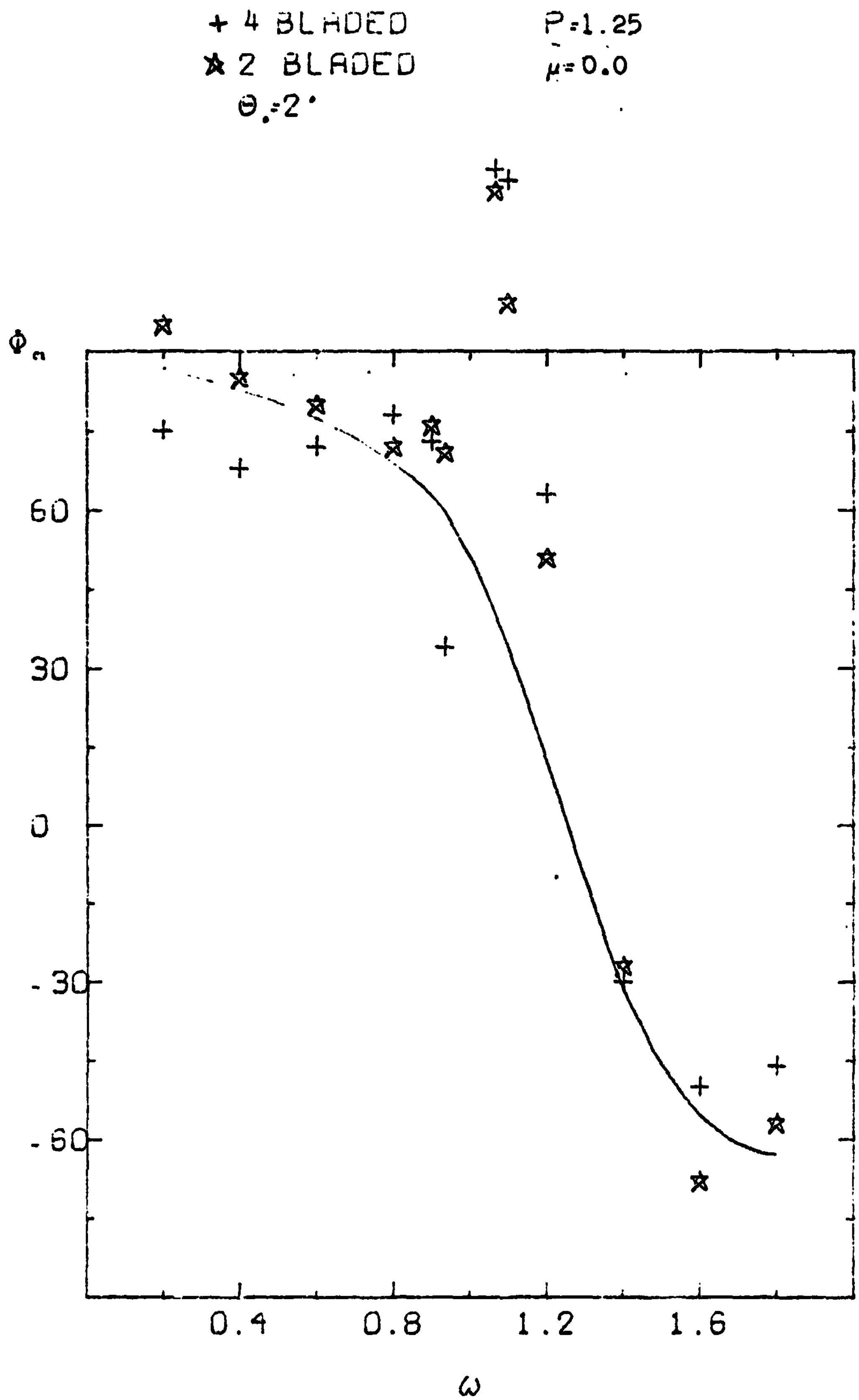

Figure 21

$\theta_0=0^\circ$ $\mu=0.0$

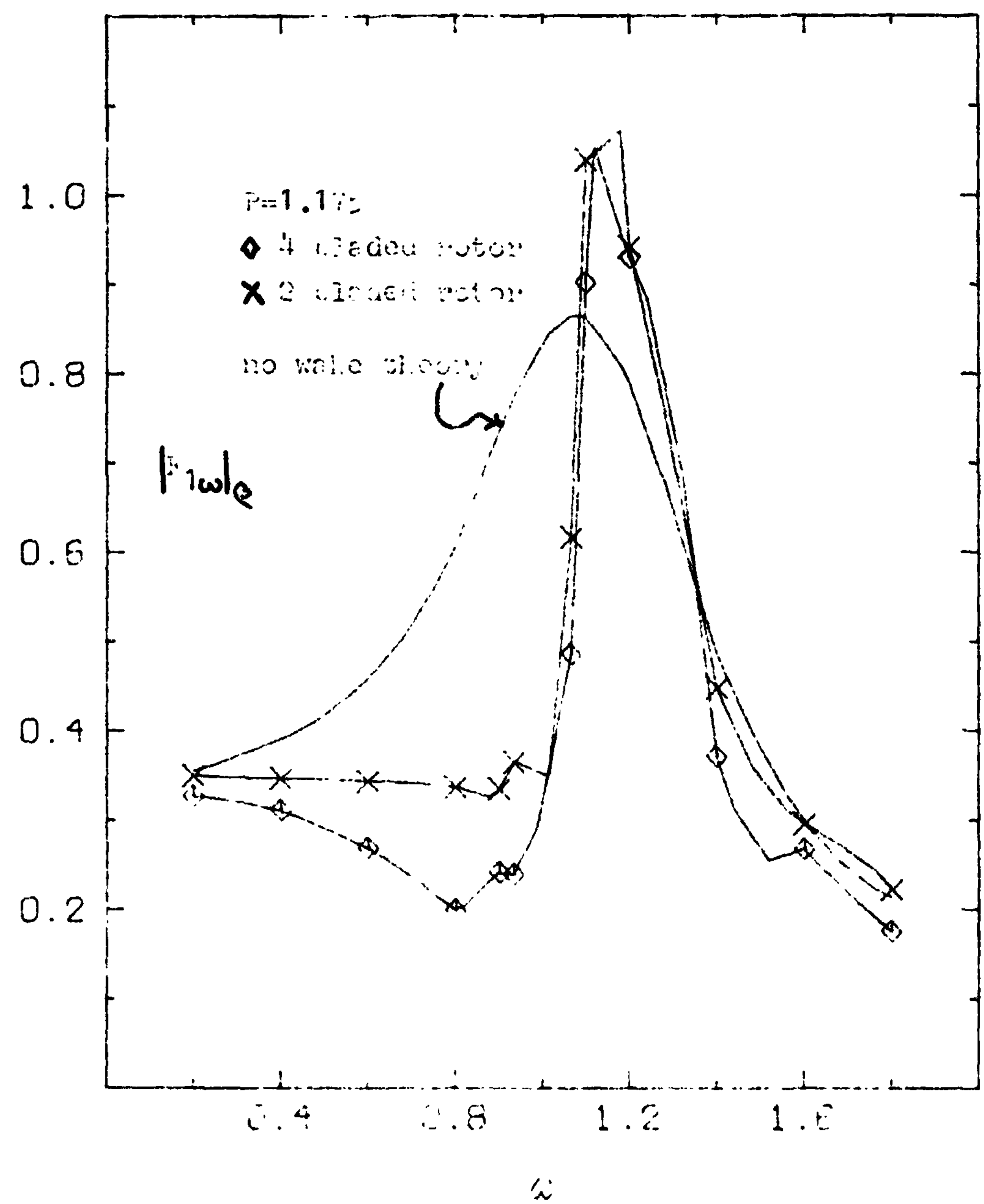

Figure 22

+ 4 bladed rotor P=1.175

☆ 2 bladed rotor

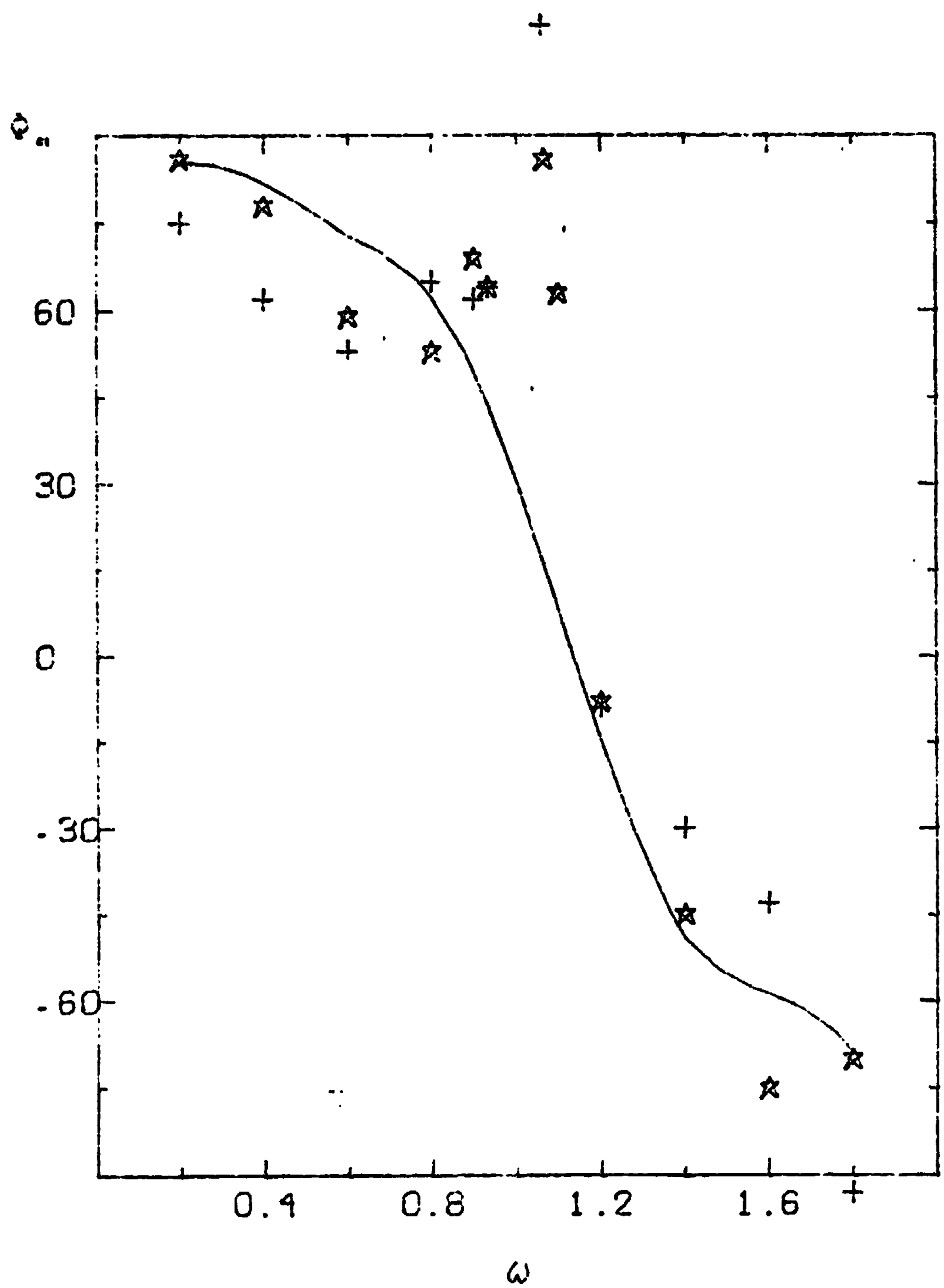

Figure 23

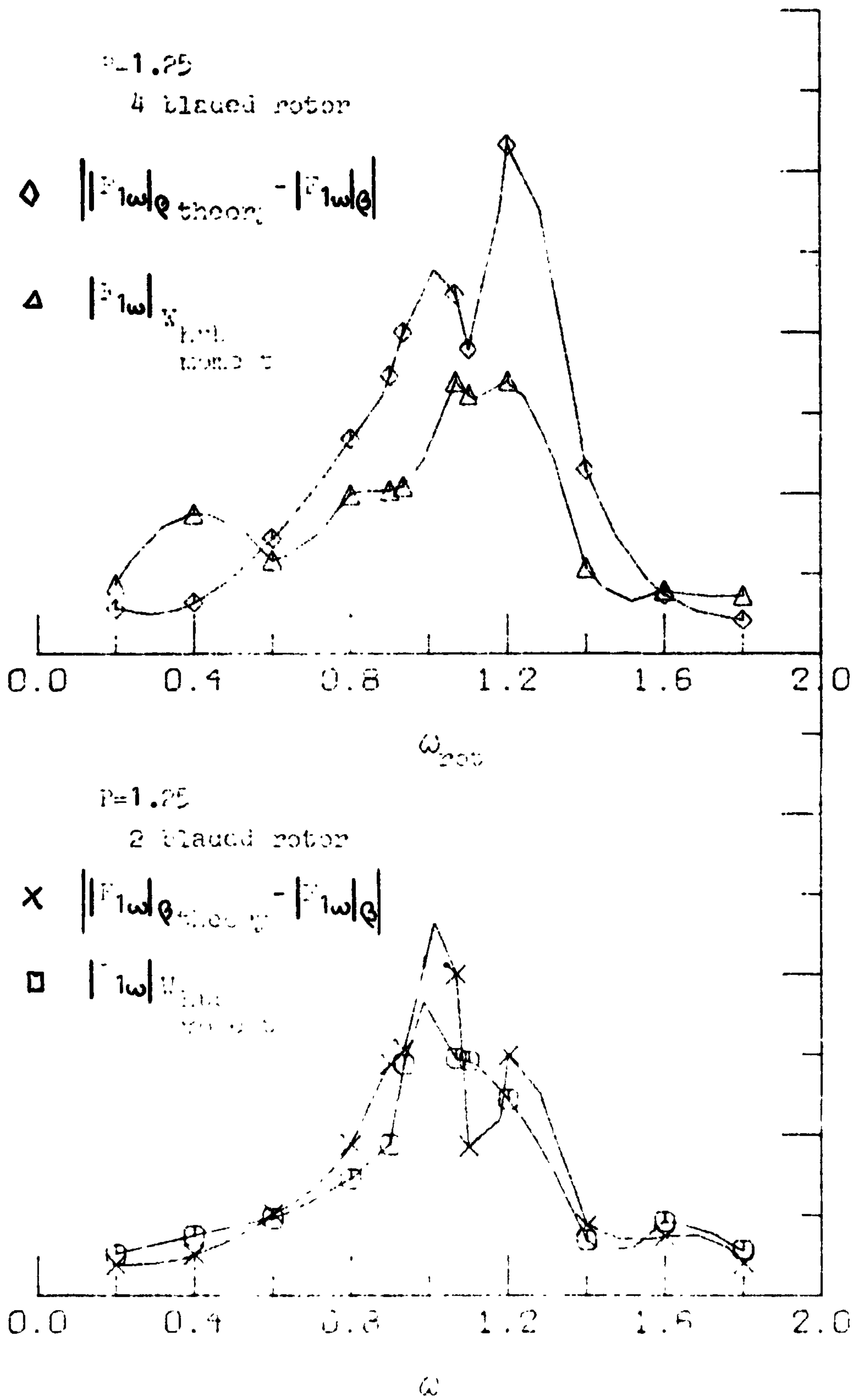
P=1.25
4 bladed rotor
0.0
0.4
0.8
1.2
1.6
2.0
ω_{rot}
P=1.25
2 bladed rotor
0.0
0.4
0.8
1.2
1.6
2.0
ω

Figure 24

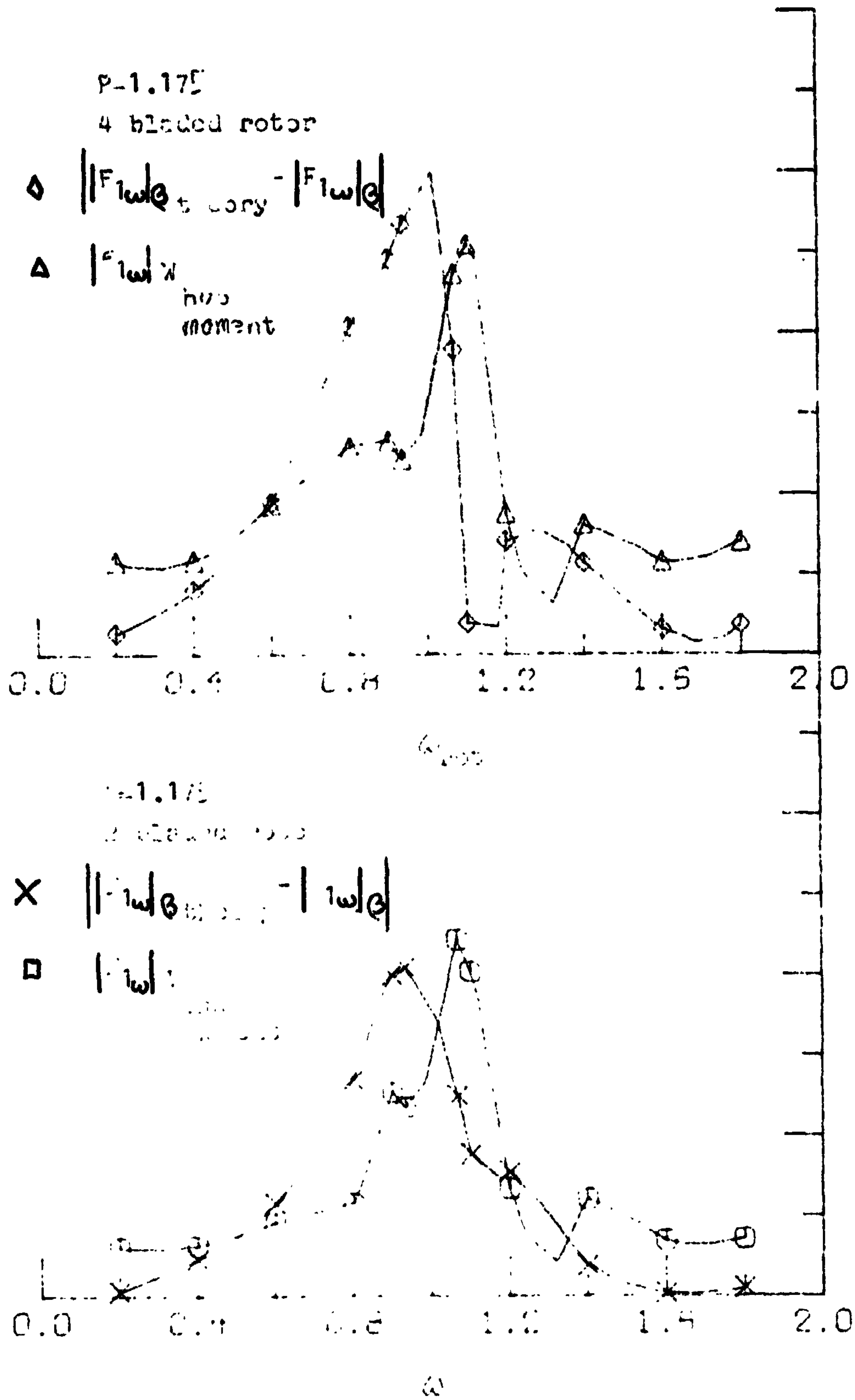

Figure [illegible]

Appendix A

List of Purchased and Borrowed Equipment

I. Equipment purchased under Contract NAS2-4151 and carried over to Contract NAS2-7613 with purchase price over $1,000.

1 - TSI Thermo Systems Incorporated Model 1050 Research Anemometer	$1,285.00
2 - TSI Model 1052 Polynomial Linearizers at $1,150 each	2,300.00
1 - TSI Model 1015C Correlator	1,075.00
SUM	$4,660.00

II. Equipment purchased under Contract NAS2-7613 over $300

1 - Digital Multimeter	$300.00

III. Borrowed Equipment - over $1,000.00

1 - TSI Single Channel, non-linearized hot wire anemometry system	$3,600.00 (New value)
2 - Tektronix Type 502A Dual Beam Oscilloscopes	$2,200.00 (New value)
1 - Ampex FR-1300 Recorder/Reproducer	$7,500.00 (New value)
1 - Hewlett Packard Thermal Recording System	$7,500.00 (New value)
1 - Consolidated Electrodynamics Corp. Type 5-124 Recording Oscillograph	$3,000.00 (New value)
1 - 2-channel adjustable high-low pass variable filter	$2,200.00
TOTAL	$27,800.00